การสังเคราะห์อนุภาคนาโนแบบลูกบาศก์เฟอริแมกเนติกแมกนีไทต์เคลือบด้วยพอลิ(2-(ไดเมทิลแอมิโน)เอทิล เมทาคริเลต)เพื่อประยุกต์ในการนำส่งยาทางทันตกรรม

นายประณต อาจคิดการ

วิทยานิพนธ์นี้เป็นส่วนหนึ่งของการศึกษาตามหลักสูตรปริญญาวิทยาศาสตรมหาบัณฑิต
สาขาวิชาปิโตรเคมีและวิทยาศาสตร์พอลิเมอร์
คณะวิทยาศาสตร์ จุฬาลงกรณ์มหาวิทยาลัย
ปีการศึกษา 2558

SYNTHESIS OF FERRIMAGNETIC MAGNETITE NANOCUBES COATED WITH POLY(2-(DIMETHYL AMINO)ETHYL METHACRYLATE) FOR APPLICATIONS IN DRUG DELIVERY IN DENTISTRY

Mr. Phranot Ajkidkarn

A Thesis Submitted in Partial Fulfillment of the Requirements
for the Degree of Master of Science Program in Petrochemistry and Polymer Science
Faculty of Science
Chulalongkorn University
Academic Year 2015

Thesis Title	SYNTHESIS OF FERRIMAGNETIC MAGNETITE NANOCUBES COATED WITH POLY(2-(DIMETHYL AMINO)ETHYL METHACRYLATE) FOR APPLICATIONS IN DRUG DELIVERY IN DENTISTRY
By	Mr. Phranot Ajkidkarn
Field of Study	Petrochemistry and Polymer Science
Thesis Advisor	Numpon Insin, Ph.D.

Accepted by the Faculty of Science, Chulalongkorn University in Partial Fulfillment of the Requirements for the Master's Degree

.....Dean of the Faculty of Science
(Associate Professor Polkit Sangvanich, Ph.D.)

THESIS COMMITTEE

.....Chairman
(Professor Pattarapan Prasassarakich, Ph.D.)

.....Thesis Advisor
(Numpon Insin, Ph.D.)

.....Examiner
(Assistant Professor Anawat Ajavakom, Ph.D.)

.....External Examiner
(Assistant Professor Chuda Chittasupho, Ph.D.)

ประณต อาจคิดการ : การสังเคราะห์อนุภาคนาโนแบบลูกบาศก์เฟอริแมกเนติกแมกนีไทต์เคลือบด้วยพอลิ(2-(ไดเมทิลแอมิโน)เอทิล เมทาคริเลต)เพื่อประยุกต์ในการนำส่งยาทางทันตกรรม (SYNTHESIS OF FERRIMAGNETIC MAGNETITE NANOCUBES COATED WITH POLY(2-(DIMETHYL AMINO)ETHYL METHACRYLATE) FOR APPLICATIONS IN DRUG DELIVERY IN DENTISTRY) อ.ที่ปรึกษาวิทยานิพนธ์หลัก: ดร.นำพล อินสิน, 64 หน้า.

การสังเคราะห์อนุภาคแม่เหล็กระดับนาโนแบบลูกบาศก์โดยใช้ไอรอน โอลิเอตเป็นสารตั้งต้น ด้วยวิธีการสลายตัวทางความร้อนที่อุณหภูมิ 290 องศาเซลเซียส ซึ่งอนุภาคที่สังเคราะห์ได้มีขนาดเส้นผ่านศูนย์กลาง 60 นาโนเมตร และมีค่าความเป็นแม่เหล็กสูง อนุภาคแม่เหล็กระดับนาโนแบบลูกบาศก์ที่สังเคราะห์ได้ถูกเคลือบด้วยพอลิ(2-(ไดเมทิลแอมิโน)เอทิล เมทาคริเลต) ผ่านปฏิกิริยาอะตอมทรานสเฟอร์แรดิคัลพอลิเมอไรเซชั่น ซึ่งมีสมบัติในการละลายน้ำได้ดี ตอบสนองต่อพีเอช และเป็นมิตรต่อสิ่งแวดล้อม ทำให้วัสดุมีคุณสมบัตินำส่งยาที่ดี กระจายตัวได้ดี มีค่าความเป็นพิษต่อเซลล์ต่ำ และควบคุมการปล่อยยาได้ นอกจากนี้ได้มีการศึกษาความเป็นพิษต่อเซลล์ของอนุภาคแม่เหล็กระดับนาโนแบบลูกบาศก์ที่เคลือบด้วยพอลิเมอร์ ด้วยเซลล์ไฟโบรบลาสต์และเซลแมคโครฟาจ ผ่านวีธี MTT assay โดยใช้ความเข้มข้นของอนุภาคแม่เหล็กระดับนาโนแบบลูกบาศก์ที่เคลือบด้วยพอลิเมอร์ 100 ไมโครกรัมต่อมิลลิลิตร ในตู้เก็บความชื้นที่อุณหภูมิ 37 องศาเซลเซียส ใต้บรรยากาศที่มีแก๊สคาร์บอนไดออกไซด์ร้อยละ 5 เป็นระยะเวลา 24 ชั่วโมง พบว่าความมีชีวิตของเซลล์มีค่ามากกว่าร้อยละ 80 อนุภาคแม่เหล็กระดับนาโนแบบลูกบาศก์ที่เคลือบด้วยพอลิเมอร์ถูกนำไปใช้เพื่อนำส่งยาอัลคาไลน์ ไฮเปอร์คลอไรท์ และปลอดปล่อยยาที่สภาวะพีเอชที่เหมาะสมได้ ในด้านการแทรกซึมผ่านฟันของอนุภาคแม่เหล็กระดับนาโนแบบลูกบาศก์ที่เคลือบด้วยพอลิเมอร์สามารถซึมผ่านฟันได้ในระยะเวลา 30 นาที ภายใต้สนามแม่เหล็กภายนอก แสดงให้เห็นว่าวัสดุนี้มีศักยภาพที่จะพัฒนาเพื่อการนำส่งยาผ่านฟันได้

สาขาวิชา ปิโตรเคมีและวิทยาศาสตร์พอลิเมอร์ ลายมือชื่อนิสิต .....

ปีการศึกษา 2558 ลายมือชื่อ อ.ที่ปรึกษาหลัก .....

5672228623 : MAJOR PETROCHEMISTRY AND POLYMER SCIENCE
KEYWORDS: MAGMETIC NANOCUBES / FERRIMAGNETIC MAGNETITE / MAGNETIC MATERIALS

PHRANOT AJKIDKARN: SYNTHESIS OF FERRIMAGNETIC MAGNETITE NANOCUBES COATED WITH POLY(2-(DIMETHYL AMINO)ETHYL METHACRYLATE) FOR APPLICATIONS IN DRUG DELIVERY IN DENTISTRY. ADVISOR: NUMPON INSIN, Ph.D., 64 pp.

Well-defined ferromagnetic magnetite nanocubes (FMNCs) with the diameter of around 60 nm were synthesized using a thermal decomposition method at 29ºC with iron-oleate complexes as starting materials resulting in nanostructure with high saturation magnetization. The FMNCs were then coated with poly(2-(dimethyl amino)ethyl methacrylate) (PDMAEMA), a water-soluble, biodegradable, and pH-responsive polymer, in order to become good drug carriers with excellent dispersity in biological buffer, low cytotoxicity, and controllable drug release. The polymer coating was performed using atom transfer radical polymerization (ATRP). Furthermore, FMNCs/PDMAEMA were studied for cytotoxicity to fibroblast and raw cells using 3- (4,5-dimethylthiazol-2-yl)-2,5-diphenyltetrazolium bromide (MTT) assay, and the result showed that FMNCs/PDMAEMA were biocompatible with those cells with cell viability of more than 80% after incubation with the highest nanocomposites concentration of 100 μg/mL for 24 h in humidified hood at 37oC and 5% CO2. The behavior of model drug alkaline hyperchlorite released from the FMNCs/PDMAEMA indicated that the drug release could be controlled by altering pH of the environment. As a result of successfully synthesized FMCNs/PDMAEMA, dentine infiltration of FMNCs/PDMAEMA was performed. It was observed that FMNCs/PDMAEMA could significantly infiltrate the dentine within 30 min under an external magnetic field, indicating the potential of these composites as transdentinal drug carriers.

Field of Study:	Petrochemistry and Polymer Science	Student's Signature	.....
		Advisor's Signature	.....
Academic Year:	2015		

ACKNOWLEDGEMENTS

First of all, I would like to appreciate that Dr. Numpon Insin, who is my thesis advisor, not only offered me magnificent assistance to successfully achieve my thesis completed, but also provided all of crucial and beneficial information and knowledge for my thesis and career in the near future.

For worthy comments and advices, I would to thank my thesis committee, Professor Dr. Pattarapan Prasassarakichassociate, Assitance Professor Dr. Anawat Ajavakom, and Assitance Professor Dr. Chuda Chittasupho. This research would have not been completed without all of their kindness. Moreover, it is an honor to have Dr. Patcharee Ritprajak who gave me a huge knowledge and guided me a way of cytotoxicity measurement and dentistry. Also, I thank you every tooth donor for the dedication.

In addition, I would also give special thanks to all of members of Materials Chemistry and Catalyst Research Unit who are always helpful. Especially, Miss Wishulada Injumpa, Miss Chalatan Saengruengrit, Mr. Sarawuth Phaenthong, Miss Padtaraporn Chunhom, Miss Radawan Palikanon, Mr. Korakot Niyomsat, and Miss Jamonpan Yangcharoenyuenyong.

For supportive assistance, I would like to give a huge thank to Mr. Tepbordin Chuaprasert and Miss Apichaya Thiangtrong for helping me about lab instrument guidance and interpretation.

Another precious group is my family who admits and supports all of everything in my life and my thesis; furthermore, they are my extreme encouragement for working on this research.

Ultimately, we would like to thank Petrochemistry and Polymer Science program, Faculty of Science, and Chulalongkorn University for laboratory facilities and instruments.

CONTENTS

Page

Page

Page

LIST OF TABLES

Table Page

LIST OF FIGURES

LIST OF FUGURES (CONTINUED)

Figure **Page**

LIST OF FIGURES (CONTINUED)

Figure **Page**

LIST OF FUGURES (CONTINUED)

Figure **Page**

LIST OF ABBREVIATIONS

FMNCs	=	ferrimagnetic magnetite nanocubes
PDMAEMA	=	poly((2-(dimethyl amino) ethyl methacrylate)
FMNCs/PDMAEMA	=	ferrimagnetic magnetite nanocubes coated with poly((2-(dimethyl amino) ethyl methacrylate)
DMAEMA	=	(2- dimethylamino) ethyl methacrylate
FMNCs-Br	=	bromine-functionalized ferrimagnetic magnetite nanocubes
PMDETA	=	pentamethyldiethylenetriamine
EBB	=	ethyl 2-bromobutyrate
OA	=	oleic acid
ATRP	=	atom transfer radical polymerization
h	=	hour
min	=	minute
g	=	gram
mg	=	milligram
L	=	liter
mL	=	milliliter

CHAPTER I
INTRODUCTION

1.1 Statement of the problems

Nanotechnology on magnetism and magnetic materials has been developed and studied extensively for the recent decades. Magnetic nanoparticles were applied in magnetic targeting, magnetic drug carriers, and diagnostic materials [1, 2]. Accordingly, the magnetic nanoparticles help drug delivery better right to the targeted position and reduces time used in the delivery systems. On the other hand, the process of synthesis and development of materials have not been extremely applied in clinical term of dentistry due to the fact that the efficacy of these materials is still diminutive and ineffective.

Currently, root canal treatment or endodontic treatment is the way to cure the pain from decayed teeth and infected pulp owing to inflammation, deep decay, repeated dental procedures on the tooth, faulty crowns, or a crack or chip in the tooth. Likewise, if pulp inflammation or infection is left untreated, it can cause pain or lead to an abscess. Thereby, infected or inflamed pulp was removed, cleansed, and later filled and sealed with a rubber-like material called gutta-percha. In the last decades, the infected or inflamed pulp would be treated by a dental extraction, which the present root canal treatment could help keep teeth on purpose. However, there are several problems in this treatment such as complex techniques, difficulties to remove and clean, and high risk for teeth brittle or breakage. In addition, it is not only high cost and long-time treatment, but it also may cause complications, side effects and death—if it is not safe and good cleaning.

In this work, the project was aimed at development of the magnetic materials for enhancing their performance in drug delivery applications. Firstly, magnetic nanocubes were accomplishedly synthesized; moreover, it exhibited an increase of higher magnetic moment, excellent saturation magnetization and good behavioral superparamagnetism leading to a better right to targeted positions by an external magnetic induction[3]. Secondly, magnetic nanocubes were coated with poly(2-

(dimethyl amino) ethyl methacrylate), a water-soluble, biodegradable, and pH-responsive polymer, in order to become good drug carriers with excellent dispersity in biological buffer, low cytotoxicity, and controllable drug release. The polymer coating was performed using atom transfer radical polymerization (ATRP).

1.2 Objectives of this thesis

1.1.1 To synthesize and characterize magnetic nanocubes with ca. 60 nm in diameter.

1.1.2 To synthesize and characterize biodegradable poly(2-(dimethyl amino)ethyl methacrylate coated onto magnetic nanocubes.

1.1.3 To study and investigate cytotoxicity and infiltration through dentin disc in applications of endodontic drug delivery.

1.3 Scope of this thesis

First of all, synthesis of 60 nm magnetic nanocubes was successfully done through thermal decomposition. Later, the biodegradable poly(2-(dimethyl amino)ethyl methacrylate was coated onto magnetic nanocubes in order to use for applications in dentistry. Moreover, study of the infiltration of the materials through dentine disc, cytotoxicity, and their drug release properties were virtually investigated in the development of drug delivery system by using magnetic nanocubes coated with poly(2-(dimethyl amino)ethyl methacrylate. For confirmation of their properties, nanocubes were characterized by transmission electron microscope (TEM), field emission scanning electron microscopy (FE-SEM) and fourier transmission infrared spectroscopy (FT-IR). Thermogravimetry analysis (TGA) was performed to confirm the polymer coating. The infiltration study was investigated by inductively coupled plasma optical emission spectrometer (ICP-OES). Likewise, cytotoxicity was virtually determined by 3-(4,5-dimethylthiazol-2-yl)-2,5-diphenyltetrazolium bromide (MTT) assay.

1.4 The benefits of this thesis

Synthesized magnetic nanocubes coated with biodegradable poly(2-(dimethyl amino)ethyl methacrylate were distinctively obtained in order to the study of

developing drug delivery applications for root canal treatment by an external magnetic induction.

CHAPTER II

THEORIES AND LITERATURE REVIEWS

2.1 Materials

2.1.1 Magnetic materials

2.1.1.1 Origin of magnetism

Magnets currently play an essential role in a modern life; as we know, a massive number of instruments are manipulated in the electromagnetic industry. In past existence human beings experienced magnetic phenomena by exploiting natural iron minerals, especially magnetite. Till modern times, magnetic phenomena were esteem apart from the viewpoint of electromagnetics, to which many physicists such as Oersted and Faraday made a vast contribution. Particularly, based on a small circular electric current, Ampère illustrated magnetic materials in 1822 that his important law brought in the concept of a magnetic moment or magnetic dipoles, similar to electric dipoles. In **Figure 2.1**, it was represented macroscopic electromagnetic phenomena where a bar magnet and a circuital current in a wire is an indicative of a physical equivalence [3, 4].

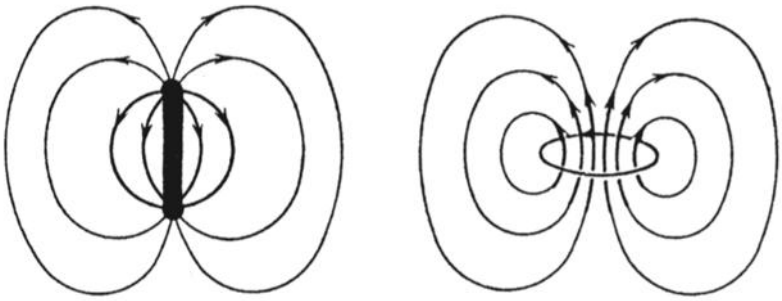

Figure2. 1 *Magnetic fields due to a bar magnet and a circuital current [2].*

Simultaneously, microscopic is exhibited in **Figure 2.2** in integral comparison of a magnetic moment or dipole and a microscopic electron rotational motion.

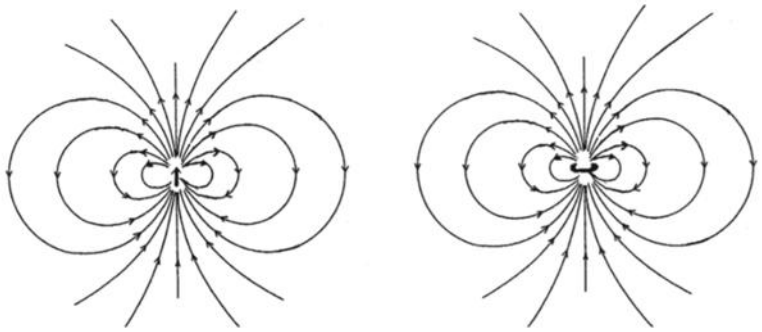

Figure2. 2 *Magnetic fields due to a magnetic moment and a small circular current [5].*

An easy way to be electromagnet is capable of being created by only wrapping copper wire into the form of a coil and linking the wire to a battery. In the coil, a magnetic field is generated; however, it remains there only whilst electricity continuously flows through the wire. In addition, the field generated by the magnet is correlated with the motions and interactions of its electron—the moment charged particles orbiting the nucleus of each atom. Electricity is of the distinctive movement of electrons, either in a wire or in an atom, thereby, each atom typifies a small permanent magnet on its own purpose. Its own orbital magnetic field was produced by the circulating electron, measured in Bohr magnetons (μB), as well as, electron spinning, like the earth, on its own axis related with a spin magnetic moment in **Figure 2.3**. Owing to the electrons being grouped in pairs, it causes the magnetic moment to be cancelled by its neighbor in most materials of which resultant magnetic moments.[6]

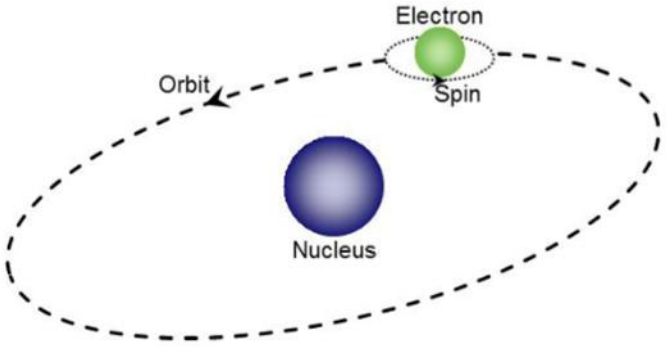

Figure2. 3 *The orbit of a spinning electron about the nucleus of an atom [1].*

2.1.1.2 Classifications of magnetic materials

As each material possesses a different property divided into main three categories: diamagnetism, paramagnetism, and ferromagnetism. Vector summation represented a whole for each magnetic moment of a molecular magnet involving atoms or ions. Magnetization, *M*, is dependent on the individual magnetic moments of its constituent magnetic origins, of which the material property is. The magnetic interaction modes at a microscopic molecular level affects the magnetization, considering the vector sum of each magnetic moment, leading to remarkable experimental behavior with respect to external parameters, for example, temperature and magnetic field. A response of the material placed in a magnetic field, *H*, is an indicative of magnetic induction, *B*. Typically, the normal relationship between *B* and *H* may be not simplified; nonetheless, it is regarded as a result of the magnetic field, *H*, the magnetization of the material, *M,* the magnetic susceptibility, χ as shown in **equation 2.1**.

$$M = \chi H \qquad (2.\ 1)$$

There are two possible ways, which is either positive or negative magnetic susceptibility, that is, $\chi > 0$ or $\chi < 0$. In the case of $\chi > 0$, it exhibits a nature behavior of paramagnetic materials; on the other hand, $\chi < 0$ displays a kind of diamagnetic materials. At low temperature, paramagnetic materials occasionally encounter magnetic phase with cooperative orderings of magnetic moments take place through exchange and dipolar interactions among them. Vector arrangement of magnetic moments specification is composed of a couple of ordering patterns. Parallel and antiparallel are types of ferromagnetic and antiferromagnetic materials, respectively.

Diagram summary is an explanation of the basic concept of the magnetic materials in a depiction of arrows of spin magnetic moments. There is no existence of magnetic moments in diamagnetic materials. Basically, each magnetic moment exploits a random orientation by thermal agitation in substances exhibiting any magnetic moments as shown in **Figure 2.4a**. Likewise, a drop of temperature is a standpoint of prominent magnetic interactions between each magnetic moment over the thermal energy in the surroundings; hence, some ordering of magnetic moment is produced below the phase transition temperature. A positive response of materials possessing any magnetic moments to magnetic field applied will affect an increase in susceptibility and permeability. A different magnitude in the magnetic moments of each antiferromagnetic interacting pair is considered in the term of weaker magnet—ferrimagnetic materials[7].

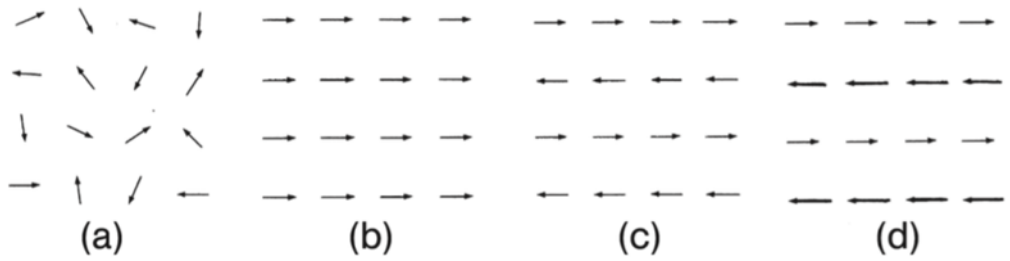

Figure2. 4 *Disordered and ordered states of magnetic moments: (a) paramagnetic; (b) ferromagnetic; (c) antiferromagnetic; and (d) ferrimagnetic [4].*

2.1.1.3 Iron oxides

Generally, there are 3 main crystalline phases in iron oxide compounds, which are comprised of magnetite (Fe_3O_4), maghemite (γ-Fe_2O_3) and hematite (α-Fe_2O_3). Accordingly, magnetite and maghemite are sorts of having ferrimagnetic property, whilst hematite exhibits an antiferromagnetic property. For magnetic application, magnetite and maghemite are of the highlight magnetic materials seeing that their magnetic properties bring a strong responses to an external magnetic field [5, 6].

2.1.1.3.1 Iron oxide nanomaterials

Small ferro/ferrimagnetic or ferro/ferrimagnetic nanoparticles exhibit a magnificent kind of magnetism that is so-called superparamagagnetism. A few nanometer to a couple of tenth of nanometers is almost the sizes in the range of superparamagnetism that impinges on the materials. In addition, these nanoparticles are made up of single-domain particles. The total magnetic moment of the nanoparticle, in a simple approximation, is able to presume as one huge magnetic moment, which is accounted for the individual magnetic moments of the atoms forming the nanoparticles. Frequently, nanoparticles play a crucial role for the direction, along which their magnetization aligns to. Anisotropy in these directions is considered as a behavior of nanoparticles property. If there is typically one preferred direction, it is defined as uniaxial anisotropy.

According to its structure as shown in **Figure 2.5**, the magnetite exhibits cubic inverse spinel structure composed of a cubic close packed array of oxide ions in which all of Fe^{2+} ions occupy half of the octahedral sites and Fe^{3+} are split evenly across the rest of octahedral sites and the tetrahedral sites. In addition to the electron spins of the Fe^{2+} and Fe^{3+} ions, the ferrimagnetism of Fe_3O_4 arises in the octahedral sites which are coupled and spin of the Fe^{3+} ions in the tetrahedral sites are coupled but anti-parallel to the former. The imbalance of magnetic contribution is of the net effect of both sets as a consequence of a permanent magnetism.

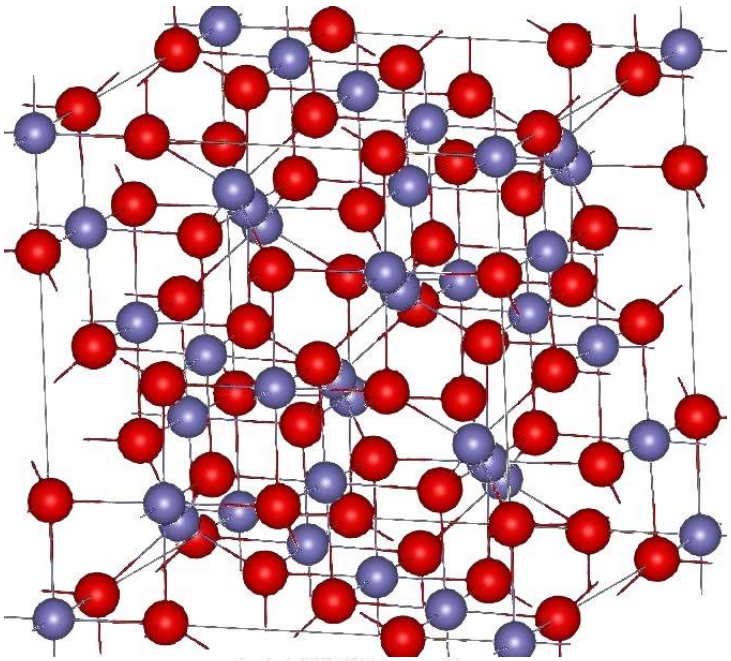

Figure2. 5 *Cubic Inverse Spinel Structure of Fe_3O_4 (magnetite) [8].*

A uniaxial anisotropy in nanoparticles nonspecifically flip the direction of their magnetization, which is triggered by thermal energy. The relaxation time related to the average time to perform such a flip is given by the **equation 2.2.**

$$\tau = \tau_0 \exp (\Delta E/k_B T) \qquad (2.2)$$

where

τ_0: The length of time characteristic of the probed material. Often it is of a magnitude of around 10^{-9} to 10^{-12} s.

ΔE: The energy barrier the magnetization flip has to overcome by thermal energy.

k_B: The Boltzmann constant.

T: The temperature.

A superparamagnetic state of nanoparticles can be observed; nonetheless, it does not only rely on the temperature T and the energy barrier ΔE:

each experimental technique corresponds with its own measurement time τ_m. The below two scenarios can happen depending on the measurement time as shown in **Figure 2.6**.

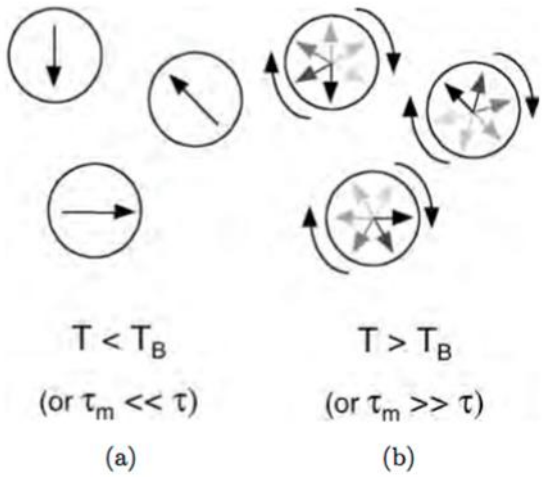

Figure2. 6 *Case 1(a): The measurement time τ_m is much smaller than the relaxation time. A well-defined state is able to be observed (block state). Case 1(b): The measurement time τ_m is much larger than the relaxation time. Owing to the fluctuating state of the magnetization, a time-averaged net moment of zero will be observed (superparamagnetic state) [3].*

$\tau_m \ll \tau$: The average time between flips is much bigger than the measurement time. This implies the particles in a well-defined state and is normally assigned to as the blocked state of the system

$\tau_m \gg \tau$: Another possible way, the average time between flips is capable of being much smaller than the measurement time. This identifies that the measurement really determined a fluctuating state with different unresolved magnetization spin directions. A time-averaged net moment of zero, as long as external field is not applied, is determined. This situation is defined as the superparamagnetic state of a system [2, 5].

2.1.2 Biocompatible materials

Biological materials are present types of natural biocompatible materials that compose a whole or a part of a living structure or biomedical device that conducts, increases, or replaces a natural function. Biocompatible materials are well known for a wide variety of applications in terms of engineering for medical, biotechnology and pharmaceutical approaches. Accordingly, biocompatibility commonly points that the material is not any causes of negative responses in the host. Determination of the potential adverse or toxic effects of a material is a factor correlated with biocompatibility. Cytotoxicity is a sign of cell killing ability or characteristics; besides, these materials are of excellent water-soluble and stable in hydrophilic solution, which also are put in for stabilizers and bio-coatings. On account of magnetic materials development used in biological application, those materials are essential to be biocompatible. Apparently, inorganic compounds and organic compounds are a current major component for synthesizing biocompatible materials. Silica, titanium, silicones and hydroxyapatite are representatives of biocompatible inorganic compounds used in synthesis. On the other hand, teflon, polyurethane, poly(ethylene glycol), poly (polyethylene glycol)methacrylate, polyamidoamine-type Dendron-b-poly(2-dimethylaminoethyl methacrylate)-b-poly(N-isopropylacrylamide) (PAMAM-b- PDMAEMA-b-PNIPAM), and poly(lactic-glycolic acid) are organic compounds used commonly [9, 10].

2.1.2.1 Biodegradable polymers

Biodegradation occurs in the sort of enzymes or chemicals deterioration correlated with living organism. Basically, the polymer fragmentation into lower molecular mass is an indication by means of either abiotic reaction or biotic reactions such as oxidation, photodegradation, hydrolysis, or degradation by microorganism. These polymers are attained from both naturally and synthetically made—particularly comprise of ester, amide and ether functional groups. Moreover, biodegradability relies not only on the origin of the polymer but also on its chemical structure and the environmental degrading conditions. To emphasize on this work, Poly((2-dimethylamino) ethyl methacrylate) (PDMAEMA) was used in coating onto a material

since it has a high reputation for being used in medical and pharmaceutical studies nowadays due to its splendid biocompatibility, hydrophilicity, and pH sensitivities. Plus, multi-functionalized materials have been gained a high interest as well. Ultimately, consideration of coating biocompatible materials and other properties such as releasing application, degradable, or loading capacity are main concerns such functionality [11].

2.1.3 Dentine and root canal treatment

Tooth mainly composes of dentine, which is supporting structure and is the second hardest tissue in the body after enamel as shown in **Figure 2.7**. The highest components are mineral and acellular, as hydroxyapatite crystal, and the rest is organic as water, collagen, and mucopolysaccharide. Inside the dentine, it is so-called dentinal tubule that is connected to the external surface along to the pulp. The diameter of dentin tubule is around 2-4 microns and roughly made up of 30,000 – 40,000 tubules per square millimeter transmitting pain to the pulp when the dentine is exposed. The hollow inner of dentinal tubules is the root or pulp canal in which this area is quite extraordinarily sensitive and grants the blood flow and nutrients that keep teeth alive.

Root canal or endodontic therapy is indicative of treatment for saving the tooth from the infected pulp of a tooth that is badly decayed or becomes infected resulting in the eradication of infection and the protection of the decontaminated tooth from future microbial invasion—the tissue surrounding the tooth will become infected and abscesses may form without treatment. Therefore, the root canal treatment is essential for the inflamed or infected pulp due to decayed and trauma teeth that save them from extraction[12].

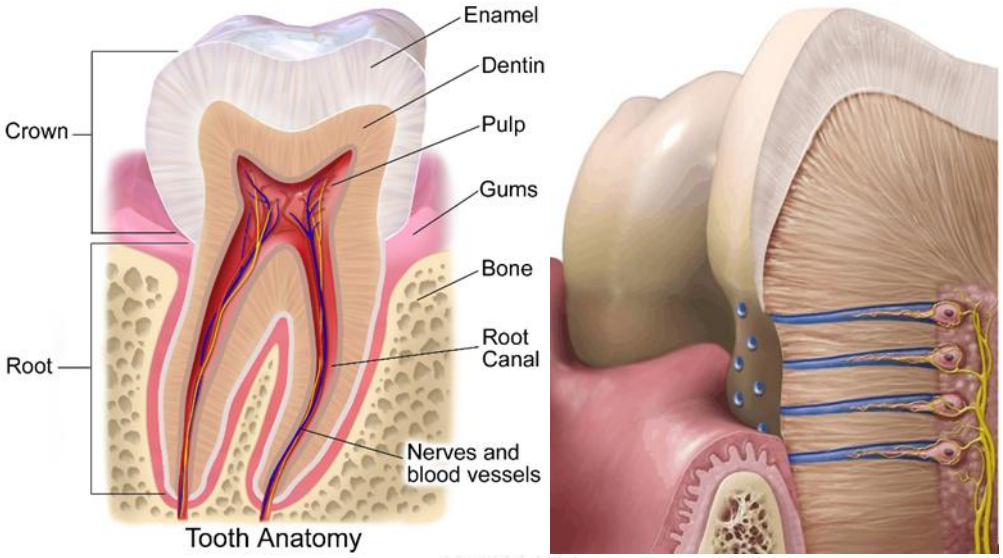

Figure2. 7 *Illustration of tooth anatomy [12].*

2.2 Principle of Synthesis

2.2.1 Magnetite nanoparticles

There are various methods used in synthesis of magnetic nanocubes, especially thermal decomposition. Thermal decomposition is one of the simple techniques that transform iron (II) and iron (III) to iron oxide at determined temperature as shown in **equation 2.3**. In addition, this technique is a marvelous reason for cost-effective preparation of iron oxide, and can control its morphology. In comparison to other techniques, production from thermal decomposition provides not only high crystallinity, but also monodispersed size particles [13, 14].

$$Fe^{2+} + Fe^{3+} + 8OH^{-} \longrightarrow Fe_3O_4 + 4H_2O \qquad (2.3)$$

Hereby, the thermal decomposition was principally employed to obtain those magnetic properties. In this recent work, iron(III) acetylacetonate was used as starting material in cooperative with oleic acid as surfactant and benzyl ether as solvent. The optimum temperature, in this process, was at 290°C to form iron oxide in

ambient air condition[15]. According to previous methods reported, there are several wide-spread starting materials used in this technique, which are a group of ferric complex such as $Fe(CO)_5$ [16], iron oleate, $Fe(Cup)_3$ (Cup = N-nitrosophenylhydroxylamine) [8], Prussian blue ($Fe_4[Fe(CN)_6$centerdot$_{14}H_2O]$ [17], Fe–urea complex ($[Fe(CON_2H_4)_6](NO_3)_3$) [18], ferrocene ($Fe(C_5H_5)_2$), and $Fe_3(CO)_{12}$ [19, 20].

2.2.2 Synthesis of polymer (ATRP)

Herein, polymerization occurred in this study is a sort of Atom Transfer Radical Polymerization (ATRP). The relationship of transition metal mediated atom transfer radical addition (ATRA) reaction, which is the main idea of this transition metal mediated controlled radical polymerization process, was formally named ATRP. Nevertheless, ATRP needs reactivation of the primarily formed alkyl halide adduct with the unsaturated compound, which is known as monomer, and the further reaction of the sporadically formed radical with additional monomer units—considered as propagation step as shown in **Figure2.8** [21].

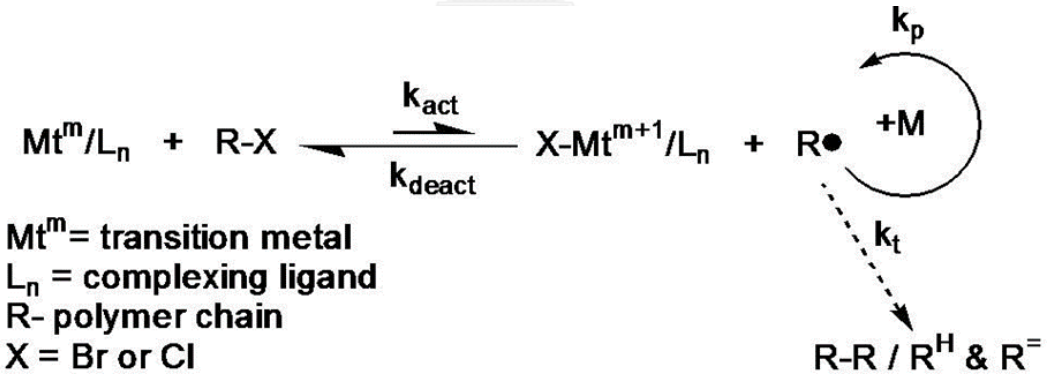

Figure2. 8 *A schematic presentation of ATRP reaction [21].*

Basically, accentuating the repetitive nature of the activation and deactivation steps and the requirement to drive the equilibrium to the left hand side are the general scheme of the ATRP equilibrium; therefore, a minute concentration of radicals to decrease radical-radical termination reactions is assembled, and a high mole fraction of dormant chains is verified. The polymerization process in ATRP related to a

complex reaction contains one or more (co)monomers, a transition metal complex in consisting of two or more oxidation states, comprising in a various number of counterions and ligands, an initiator with radically relocating atoms or groups, and an alternative solvent or a wide variety of additives. According to **Figure 2.9**, the initiator is mostly an alkyl (pseudo)halide that can be either a low or high molar mass compounds or even partially insoluble materials; for example, initiators are fixed onto their surface of modified particles, flat, wafers, or even fibers [1, 22].

Previously popular metal complex was copper as an outstanding transition metal, but there is a widespread extent of other metals introduced in ATRP involving Ti, Mo, Re, Fe, Ru, Od, Rh, Ni, and Pd that can be soluble in the reaction.

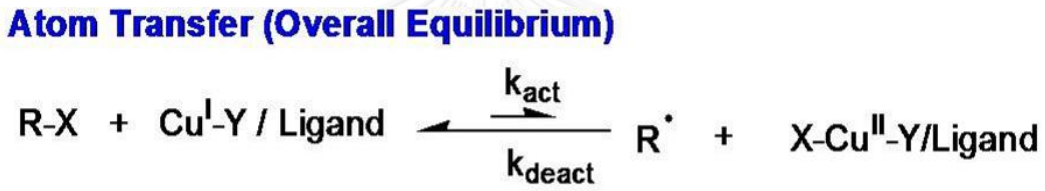

Figure2. 9 *A schematic presentation of ATRP overall equilibrium* ***[21].***

2.3 Drug delivery

As synthesized biodegradable polymer coated onto nanocubes, the main application in this research is to introduce and generate drug delivery system for new clinical aspect in dentistry application. Drug delivery system is a beneficial tool to serve the right problems in aspects of a reasonable cost and a technical usage. Yet, drug delivery in nanoparticles materials has the same trend to magnetic separation [23]. The magnetic particles and the drug will be bound or stuck together, which is later induced with external magnetic field, as a consequence of path of the tagged particles changed. At the right position, the releasing of drug will be generated from its carrier either via enzymatic activity or physiological changes such as pH, osmolality, and temperature. As previous concern, nanoparticles can completely undergo circulatory system in the body. Seemingly, tremendous advantages of targeted drug delivery are currently utilized. Targeted delivery can verify that a little amount of drug can be successfully administered at the particular areas in controlled manners [24, 25].

2.4 MTT assay and cytotoxicity studies

A response of cell population, on external factors, depends on the basis of abundant *in vitro* assays of cell viability and proliferation measurement—as stated in **Figure 2.10** identifies various reagent used for cell viability detection. Accordingly, they are depended on diverse cell functions such as enzyme activity, cell membrane permeability, cell adherence, ATP production, co-enzyme production, and nucleotide uptake activity. Many have established methods such as Colony Formation method, Crystal Violet method, Tritium-Labeled Thymidine Uptake method, MTT, and WST methods used for counting the number of live cells. To determine a reliable way of cell proliferation in this work, reduction of tetrazolium salts is evidence of the phenomenon and ubiquitously agreed as the confirmative result of it. The reduction of the yellow tetrazolium MTT (3-(4, 5-dimethylthiazolyl-2)-2, 5-diphenyltetrazolium bromide) is performed by metabolically active cells as shown in **Figure2.11**, as a consequence of the action of dehydrogenase enzymes of which produces reducing equivalents such as NADH and NADPH. Then, the intracellular purple formazan arises from being solubilized and quantified by spectrophotometric means. For easy comprehension, in this work, the more purple generated identifies the higher cell aviability—such an environmental friendly materials [1, 26-29].

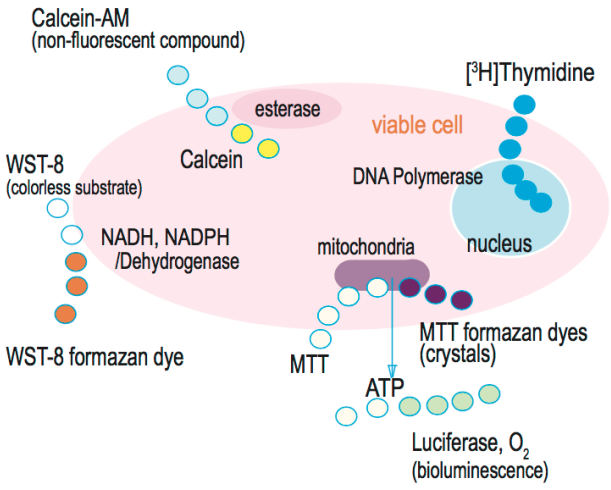

3].

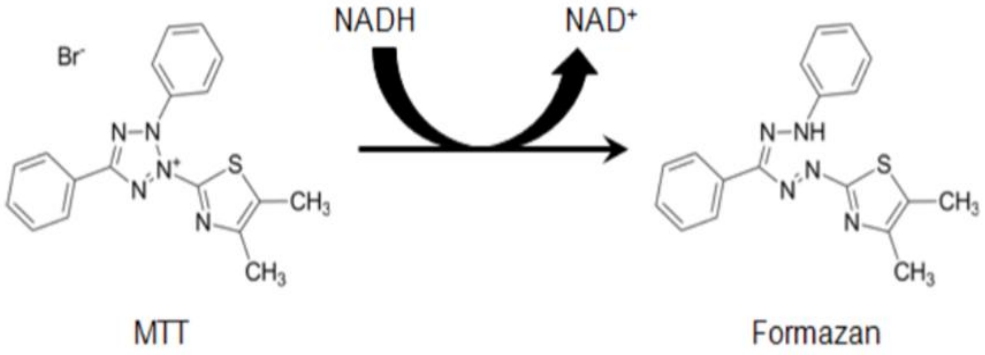

Figure2. 11 An illustrating reduction of MTT to form purplish Formazan [29].

2.5 Cell culture

To prove that our materials are not harmful to the cell, cytotoxicity is of an indicative method used in this study. Particularly, good cells must be concerned and cultured, and be kept in optimum condition for cell incubation on account of effective results. Cell culture apparently deals with the cells removal from an animal or plant and their subsequent growth in a suitable artificial environment. Before cultivation, it needs cell removal from the tissue speedily and disaggregated by enzymatic or mechanical ways. Another way of cell culture is obtained from a cell line or cell strain that has promptly been initiated.

Primary culture is the step of the culture after cell detachment from tissue and multiplication under suitable conditions till them take up all of the accessible substrate—possessed optimum confluence. Subsequently, cell passage must be drawn attention in this stage, subculture, for cell proliferation by transferring those to a new container with fresh growth media to issue more room for keeping on growth.

Hereafter, subculture referring to the primary culture will be converted into a cell line or subclone. For cell line, a life span of the primary cultures is limited as they are transferred to a new vessel. Those cells will exhibit genotypic and phenotypic uniformity in the population derived from the high growth capacity predomination. Accordingly, culture conditions depends on each cell type; on the other hand, the

imitative environment where the cell culture are produced at clean and appropriate containers comprising a substrate or media that provides the important nutrients: such as amino acids, carbohydrates, vitamins, and minerals, growth factors, hormones, and gas incubation (O_2 nd CO_2), and adjustment of the physiochemical environment (pH, osmotic pressure, temperature) [27, 30, 31].

2.6 Literature reviews

2.6.1 Applications of magnetic materials

As previously numerous studies of scientific researches, nanotechnology on magnetic nanoparticle has been obtained a high attention through this recent decade due to its versatile applications on the ground of medical and clinical uses. In order to utilize the property of magnetic applications, coating with biodegradable polymer or other surfactants by account of toxicity diminution and drug loading is mostly concerned. One of the most popular magnetic applications is about nanoparticles for sustained delivery of anticancer agents and clinical usage. Herein, magnetic nanoparticles are coated with oleic acid and pluronic acid entrapped with drug onto their surface to against the cancer cells resulting in better impact of treatment as shown in **Figure2.12**. For drug delivery system, the modified surface of magnetic nanoparticles is commonly conjugated with drug such as Doxorubicin (Dox) in the mean of cancer treatment via click reaction as shown in **Figure2.13** [32-35].

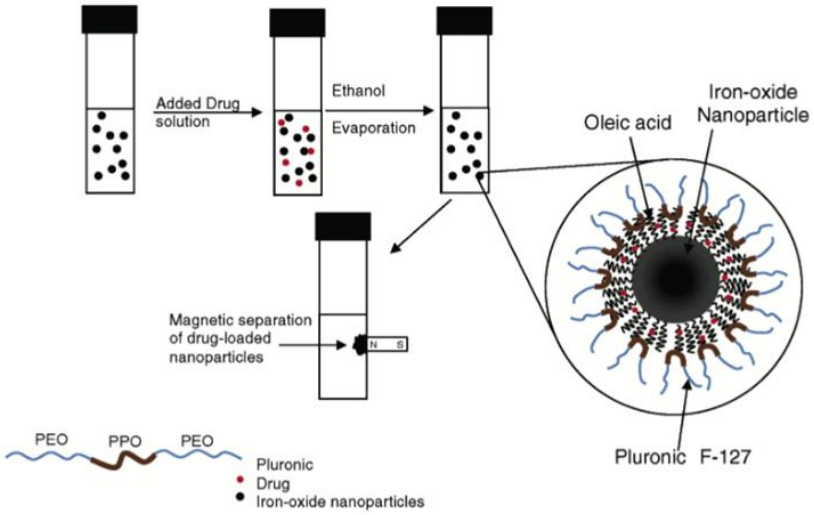

Figure2. 12 *Schematic representation of formulation of iron oxide nanoparticles and the process for drug loading [33].*

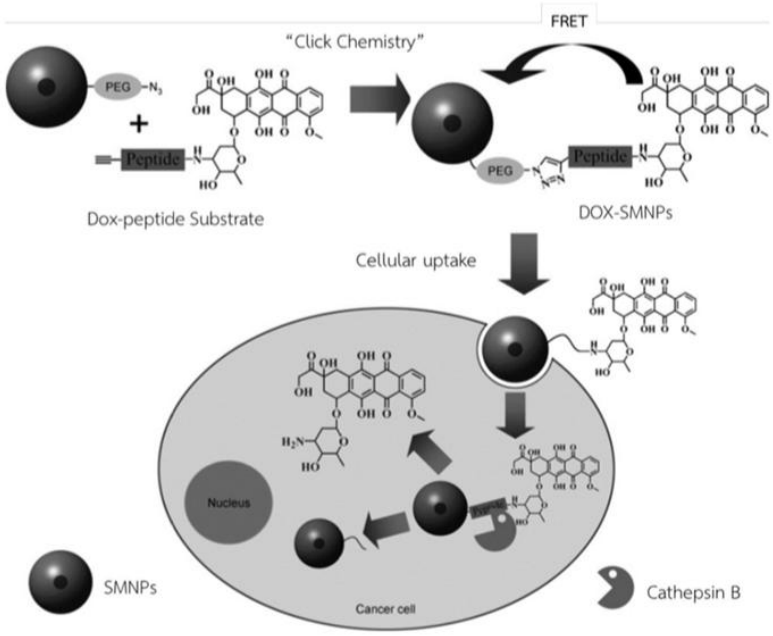

Figure2. 13 *Illustration of synthesis of Dox SMNPs and their cellular functions for drug release and tumor imaging. FRET=fluorescence resonant energy transfer [33].*

For optimized magnetic advantages, the development of magnetic nanoparticles plays a vital role to the recent study seeing that shape does matter the magnetic properties. For the morphology tailoring of inorganic nanocrystal, focusing on shape control, solvothermal polyol process is a kind of method used to gain desired

purposes by tuning the surfactants. To illustrate, iron oxide nanocubes were synthesized by using oleic acid as surfactants to multiply the concentration of free oleate ions improving the surfactant effect; furthermore, the ratio of oleic acid to oleyamine and Fe precursors was investigated. Moreover, the shape and size changes can alter the magnetic properties such as saturation magnetization in the fact that the bigger sizes of magnetic nanoparticles exhibits the higher magnetization. Specifically, the 60-nm-size of magnetic materials contains apparently 95% of bulk value; nonetheless, the larger size is significantly indicative of non-dissimilated magnetic value as shown in **Figure2.14** [7, 36, 37].

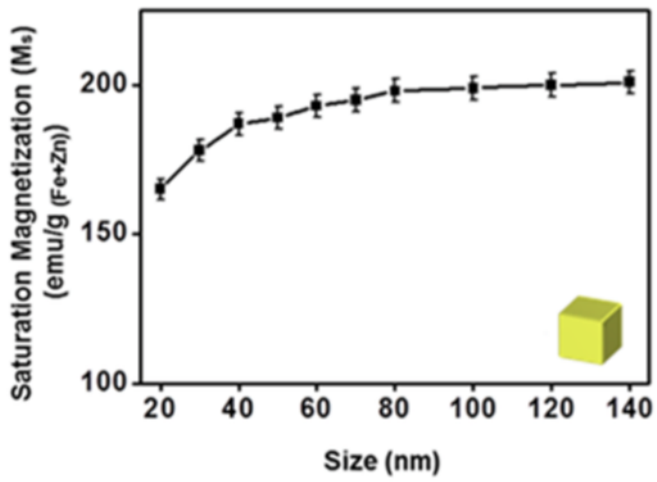

Figure2. 14 *Saturation magnetization of size tuned cube nanoparticles: M_s vs nanoparticle size [7].*

2.6.2 Synthesis and coating of PDMAEMA onto materials

Currently, coating of nanoparticles with polymers has a wide variety of benefits such as biocompatibility, biodegradability, drug loading capacity improvement, and drug delivery enhancement. In this field, polymer coating or functionality has the main purpose to enhance the drug loading capacity and help drug delivery system in a magnificent manner. As a synthesis of polymers and study of clinical applications, poly(2-(dimethylamino)ethylmethacrylate is defined as excellent polymer that can be biodegradable, drug release control, and show pH-responsive behavior due to their

tert-amino group containing in which can be protonated by altering environmental pH values. To complete polymer coating as shown in **Figure2.15**, ATRP is brought for grafting the polymer onto magnetic surface by using alkyl halide group as initiator, and can be further entrapped for an application of drug loading [21, 23, 38-40].

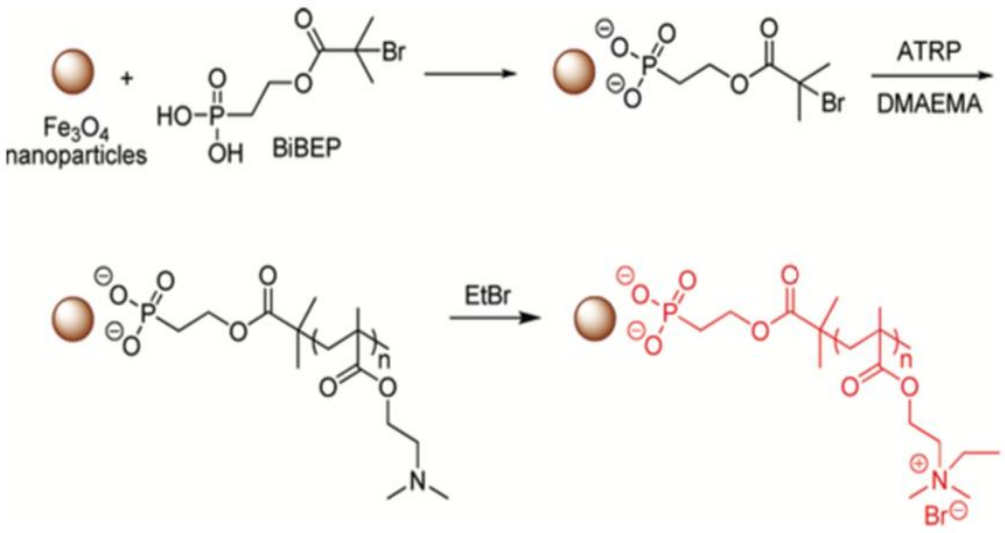

Figure2. 15 *A schematic representation of PDMAEMA coating onto magnetic nanoparticles [9].*

2.6.3 Infiltration of dentine discs

Due to the fact that drug diffusion through dentine tubules or pulp, it is evidently influenced by dentinal fluid that matters the dentine infiltration purpose and clinical importance. The investigation of dentine infiltration primarily includes two techniques, which are iontophoresis and pressure techniques as formerly reported [41-43].

First of all, iontophoresis, so-called ion delivery, is a technique that ion flow diffuses to driven media by an applied electric current. The ions will drive through dentinal tubules into the pulp, which is ionized for delivering drug. Accordingly, the technique could intensify a benefit of ionized drug for both intact and caries-affected dentine as shown in **Figure 2.16.** As a new experiment, the set-up for this ionized drug delivery system was created for study of dentine infiltration that mimics the virtually

ambient condition of dentinal tubules, as by conducting hydraulic measurement, used for only *in vitro* study as in **Figure 2.17** [44].

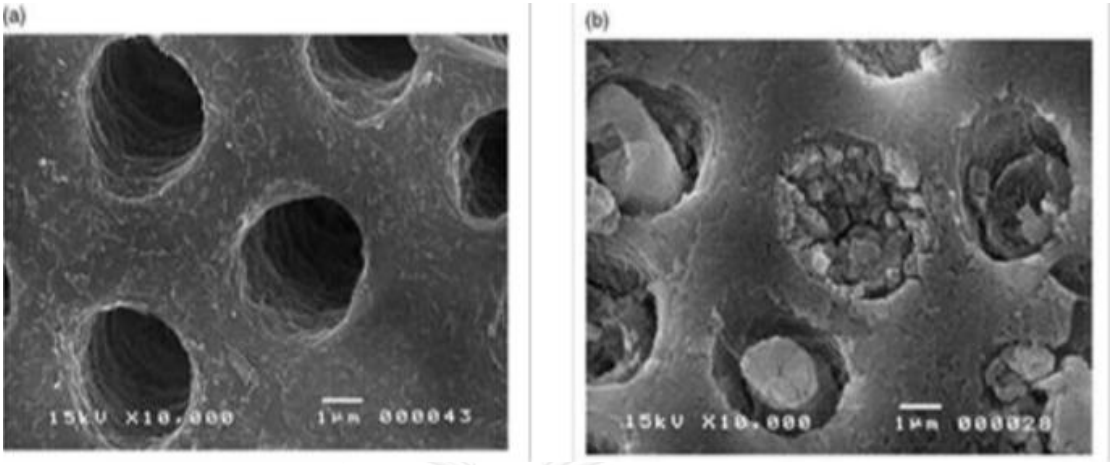

Figure2. 16 *(a) Scanning electron micrograph of intact dentine surface showed opened dentinal tubules (b) Scanning electron micrograph of caries affected dentine surface occluded dentinal tubules[44].*

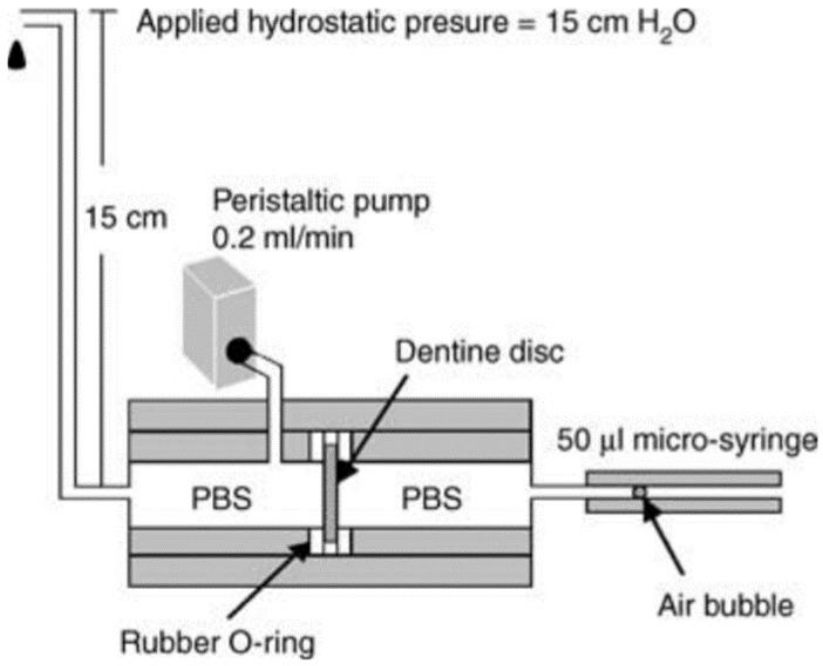

Figure2. 17 *Diagram of the experimental system for hydraulic conductance measurement (PBS, phosphate bu¡ered saline) [45].*

For second technique reported is known as the Pressure technique. As a drug delivery system, pressure diffusively flows into dentinal tubules of which it is trapped a sort of antibacterial nanoparticles conducted by using high-intensity focused ultrasound (HIFU). The HIFU, in this case, consequently is a process of collapsing cavitation bubbles in the mean of pumping action. As an expressive design, the experiment set-up in the purpose of delivering antibacterial nanoparticles into dentinal tubules as depicted in **Figure 2.18.** Subsequently, discharging a capacitor is to produce the spark bubbles, and further apply HIFU induced by voltage applier. The higher pressure pressed the bubbles after the various pressures created at which a pressure lower than liquid media was affected. The antibacterial nanoparticles in the media were finally submerged into dentinal tubules as stated in **Figure 2.19**. Above all, difficulty of dentine infiltration through dentinal tubules or dentine discs is the blockage and aggregation of antibacterial nanoparticles as shown in **Figure 2.20**, and high pressure introduction or HIFU application limited the use of this technique that would be extraordinarily observed in the upcoming research [43, 46, 47].

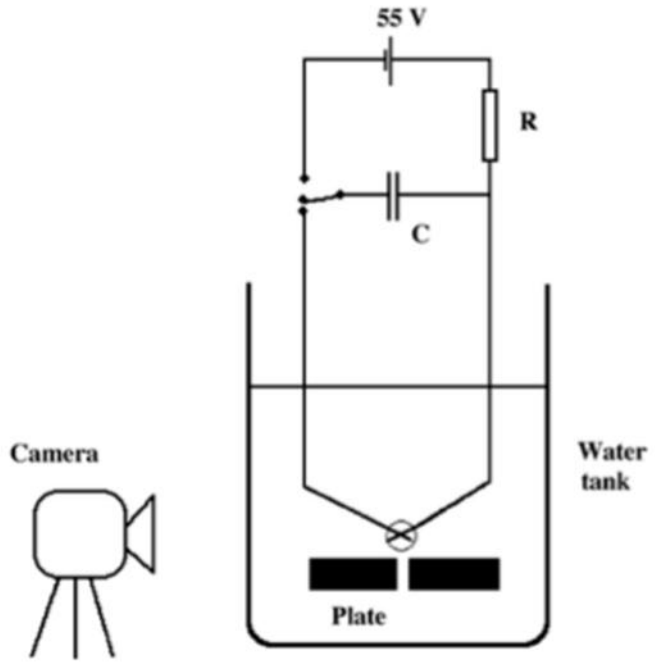

Figure2. 18 *Experimental set up of the spark-generated bubble near a plate[43].*

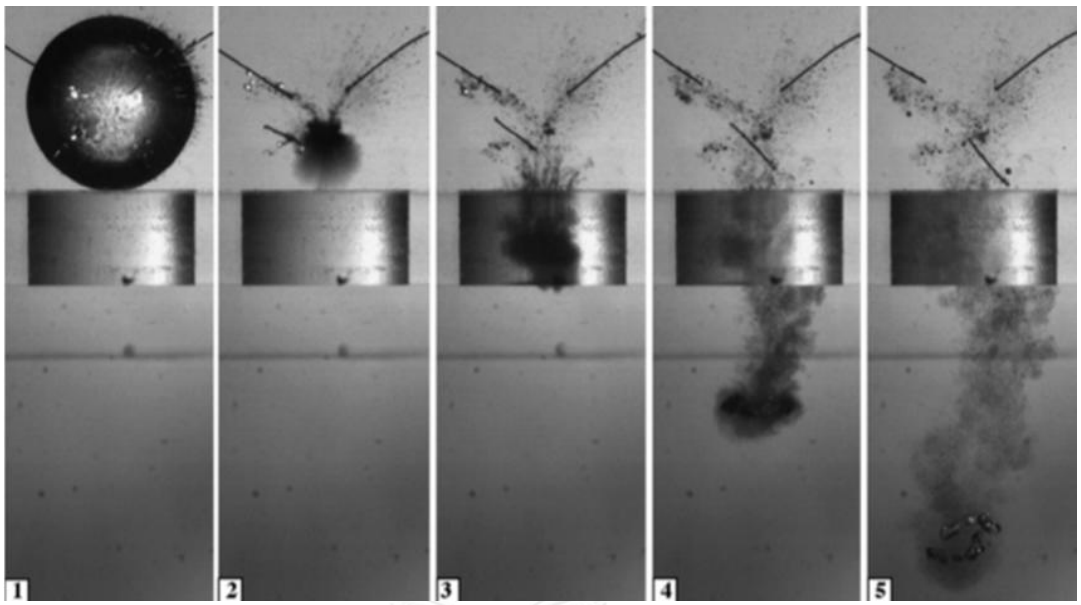

Figure2. 19 *Bubble shapes with* H′ *= 1.01 and* Rm *= 4.61 mm near a plate with a hole diameter of 9.0 mm at times (in ms) 0.88, 1.52, 2.64, 4.96 and 8.80. Note the formation of a toroidal bubble-ring in the last image. The toroidal bubble is moving downwards with a velocity of 1.5 m/s in the last image. The frames are numbered in chronological order [46].*

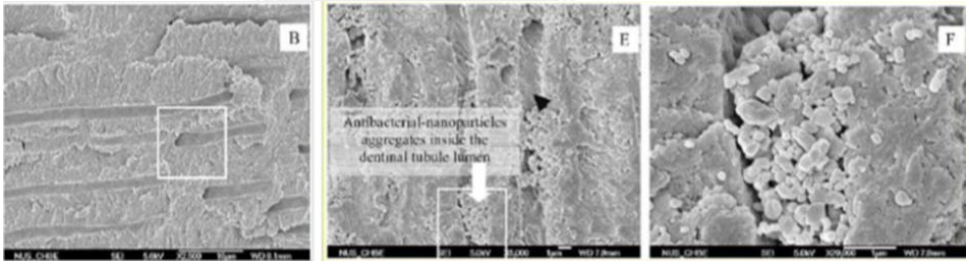

Figure2. 20 (a) The cross-section of the dentine samples with the exposed dentinal tubules did not show antibacterial-nanoparticles within the lumen, (b) Field Emission scanning electron micrographs of dentinal tubules from the HIFU treatment group samples and (c) the aggregation of antibacterial nanoparticles of 100-200mm [46].

Chapter III
EXPERIMENTS

The experimental section is divided into three parts. First part is the synthesis of 60 nm magnetic nanocubes, second part is the synthesis of poly(2-(dimethylamino)ethylmethacrylate) onto magnetic nanocubes, and the last part is the study of infiltration through dentine disc and drug release properties of the magnetic nanoparticles coated with poly(2-(dimethylamino)ethylmethacrylate).

The instrument and chemicals, which are used for the synthesis of magnetic nanocubes, the synthesis of poly(2-(dimethylamino)ethylmethacrylate), and the study of their infiltration through dentine discs and drug release properties, were listed below.

3.1 The instrument

Table3. 1 *List of instruments*

Characterization techniques	**Models**
X-ray powder diffraction spectrometer (XRD)	DMAX2200/Ultima+ (Rigaku)
Transmission electron microscope (TEM)	JEM-2100 (JOEL)

Fourier transform infared spectrometer (FTIR)	Impact 410 (Nicolet)
Inductively Coupled Plasma Optical Emission Spectrometer (ICP-OES)	Perkin Elmer Optima 2100
Scanning electron microscope (SEM)	JSM-5410
Centrifuge	Centaur 2 (Sanyo)
Magnetic stirrer	MS 101 (Gem)
Thermogravimetric analyzer (TGA)	Pyris 1 TGA (Perkin Elmer)

3.2 Chemicals

Table3. 2 *List of chemicals*

Chemicals	**Supplier**
Iron (III) acetylacetonate ($Fe(acac)_3$, 98%),	Aldrich
Oleic acid (OA, 90%)	Aldrich

Benzyl ether	Aldrich
2,2′-bipyridine (bpy, 99%)	Aldrich
α-Bromoisobutyric acid (BIB)	Aldrich
Alkaline hypochlorite	Aldrich
3-(4,5-dimethylthiazol-2-yl)-2,5-diphenyltetrazolium bromide (MTT)	Life Technologies
Dimethyl sulfoxide (DMSO)	Amresco
Toluene	Panreac
Hexane	J.T.Baker
Chloroform	J.TBaker
Ethanol	J.TBaker
THF	J.TBaker
2-(Dimethylamino)ethylmethacrylate (DMAEMA, 98%)	Aldich

3.3 Synthesis of ferrimagnetic magnetite nanocubes (FMNCs).

The desired size of 60 nm FMNCs was synthesized by thermal decomposition at optimum conditions. Accordingly, determining the amount of solvent, benzyl ether, and time used for thermal decomposition were significantly investigated and resulted in the size series of FMNCs as shown in **Figure3.1**.

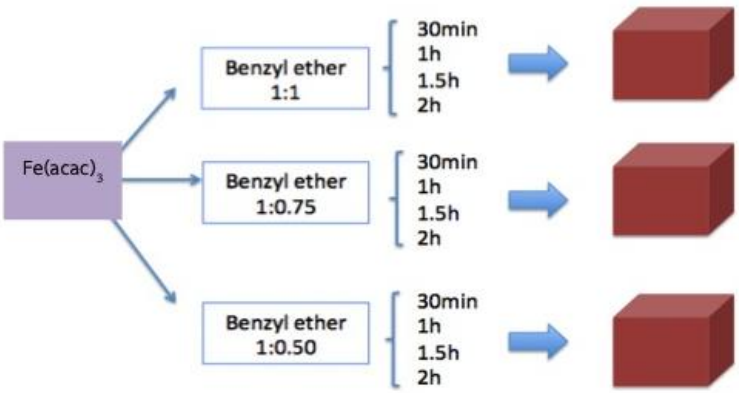

Figure3. 1 *A schematic presentation for the synthesis of magnetic nanocubes by varying solvents and time.*

Basically, the synthesis of FMNCs is composed of two main reactions as stated in **Equation 3.1**.

$$Fe(C_5H_7O_2)_3 + 3Na(OOC_{17}H_{33}) \longrightarrow Fe(OOC_{17}H_{33})_3 + 3NaC_5H_7O_2$$

$$Fe(OOC_{17}H_{33})_3 \xrightarrow{\text{Thermal Decomposition}} Fe_3O_4\ NCs$$

(3. 1)

For the synthesis of monodispersed FMNCs, firstly, iron acetylacetonate (2 mmol, 0.71 g) as starting material was added into a mixture of oleic acid (4 mmol, 1.13 g) [48] and benzyl ether (52 mmol, 10.4 g). A mixture was degassed for an hour at 60°C. Then thermal decomposition was further applied by heating a mixture to 290°C at the rate of 20°C per minute under vigorous magnetic stirring according to the temperature

proggram as shown in **Table 3.3**. The reaction was maintained at this temperature for an hour. Then, cooling to room temperature was required, and the mixture was washed with toluene and hexane (1:1). Black precipitate was attained by centrifugation and decanted by magnet separation, and the product was washed with chloroform for at least three times to obtain FMNCs [49].

Table3. 3 *Temperature program for the preparation of monodispersed ferimagnetic magnetite nanocubes (FMNCs)*

Step	Temperature (ºC)	Duration (min)	Condition
1	80	10	Vacuum
2	80	60	Vacuum
3	80-100	1	Vacuum at rate 20ºC/min
4	100-290	11	Under air at rate 20ºC/min
5	290	60	Under air
6	50	5	Under air

After determining the amount of solvent and time used, the 60 nm FMNCs were synthesized and further coated with PDMAEMA.

3.4 Synthesis of PDMAEMA modified magnetic nanocubes (FMNCs/PDMAEMA).

There are many ways to polymerize, as different initiators and various catalysts used, and coat polymer onto FMNCs. In this study, two main routes as shown in **Figure 3.2** were brought to observe the differences; likewise, the conditions were varied into 4 pathways as in **Figure 3.3** below to observe the differences in products obtained.

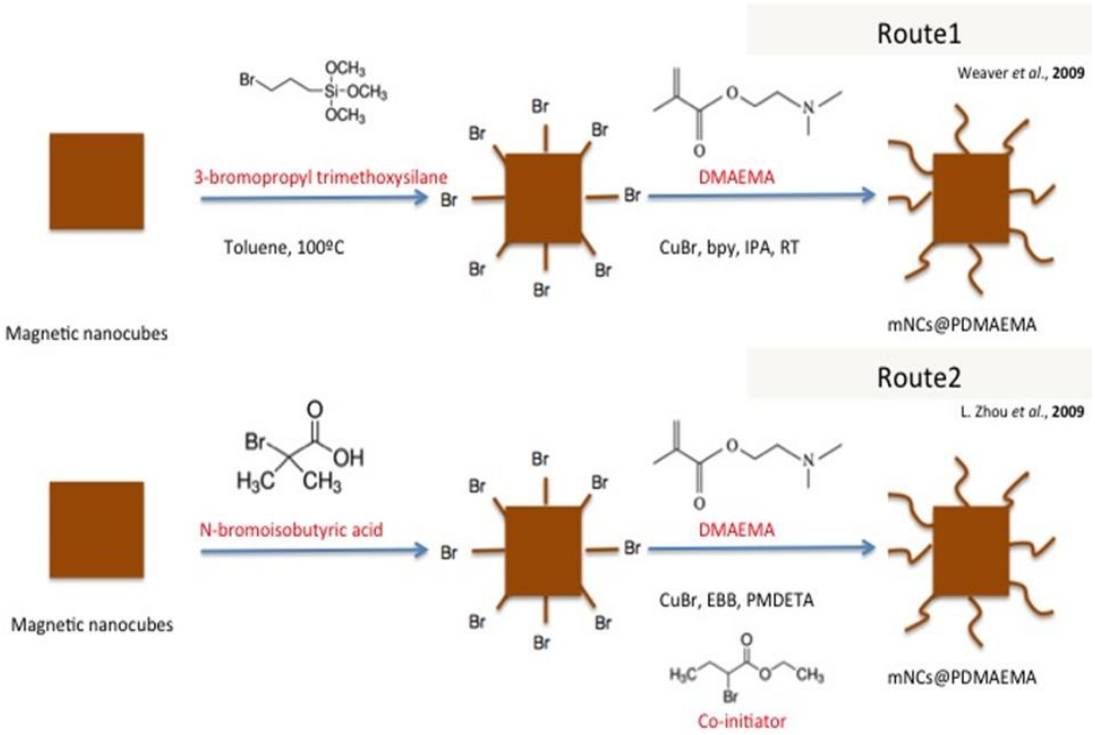

Figure3. 2 *A schematic presentation of the synthetic routes for polymer coating.*

Firstly, hydrophilic ferimagnetic magnetite nanocubes (FMNCs) with average diameters of 60 nm were functionalized using 3-bromopropyl trimethoxysilane to provide surface coverage of bromopropyl initiating groups. Atom transfer radical polymerisation was used to polymerize (2-dimethylamino)ethylmethacrylate (DMAEMA) monomer from the surfaces thus rendering the FMNCs oleophilic. Hence, FMNCs (1 g) were dispersed into toluene (50 mL) using sonication (5 min). An excess of 3-bromopropyltrimethoxysilane (1.5 mL) was slowly added, and the mixture was sonicated for another 5 min. The reaction mixture was then refluxed overnight using mechanical stirring. The bromine-functionalized nanoparticles (FMNCs-Br) were collected using a permanent magnet (decantation), followed by washing with acetone for at least 3 times and drying under vacuum. Then, isopropanol (10 mL) was used to disperse FMNCs-Br (50 mg) using ultrasonic agitation for 2 min. For polymerization step, DMAEMA monomer was added into the mixture then degassed, and copper (I) bromide

(0.1g) and bipyridyl (0.33 g) were used as catalyst and ligand in the system. The degassed mixture was sealed and stirred at room temperature overnight. Finally, the PDMAEMA-modified FMNCs was decanted and washed with water, ethanol, and hexane respectively [50].

For second route, there are correlated two steps in the method: synthesis of N-bromoisobutyric acid-functionalized magnetite nanoparticles (FMNCs–Br), and synthesis of FMNCs/PDMAEMA.

First of all, the FMNCs suspension was vigorously stirred with 1.67 mmol (277.2 mg) of BIB per gram of FMNCs for 24 h at room temperature, and the particles were washed continuously with methanol and dried under vacuum at room temperature. After synthesis of FMNCs-Br, 0.3g of functionalized nanocubes and 5mL of DMF were brought in a dried flask. Later, 30 mmol of DMAEMA as monomer, 0.5 mmol of EBB (ethyl 2-bromobutyrate) as co-initiator, 0.5 mmol of CuBr, and 0.5 mmol of PMDETA (pentamethyldiethylenetriamine) as the catalyst and ligand were added. The polymerization was begun by stirring and heating the reaction mixture at 90°C for 24 h under a nitrogen atmosphere. The formed polymer coated onto FMNCs were washed with THF, and dried under vacuum at room temperature. Ultimately, the PDMAEMA homopolymer was separated by precipitation in excess petroleum ether, and dried under vacuum at room temperature [51].

To obtain best yield for the synthesis of FMNCs/PDMAEMA, the two of the initiators, in these criteria, are varied with both polymerization routes to optimize the polymer coating.

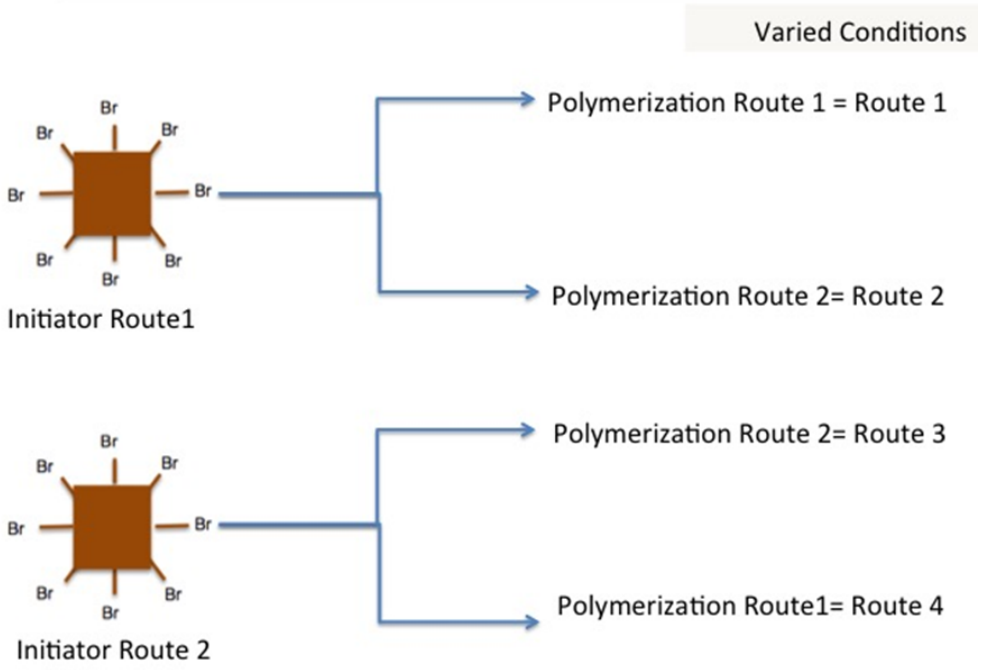

Figure3. 3 *A schematic presentation of the varied conditions of initiator for synthesis of polymer.*

Notwithstanding, there were some conditions applied after previously varied conditions to gain thicker polymer shell. Hereinafter, functionalization of dopamine onto FMNCs surface for more surface interaction was investigated as shown in **Figure 3.4.** Also, atom transfer radical polymerization (ATRP) was used to synthesize PDMAEMA onto FMNCs in this route. Dopamine (1.3 mmol, 250 mg) was added with iron oxide (FMNCs/OA, 0.09mmol, 60 mg) to form amino group on its surface [52]. The mixture was dispersed in 3 mL of DMF and stirred for 45 min. Black precipitate was isolated with a magnet and rinsed with ethanol for at least three times. α-Bromoisobutyric acid (1.67 mmol, 277.2 mg) was added and stirred for 24 h at room temperature. A solution was washed with methanol and dried under vacuum at room temperature overnight to form an initiator group on FMNCs surface. The PDMAEMA polymer was favorably synthesized; briefly, magnetite with initiator (5mmol, 50 mg) was dispersed in isopropanol (0.2mmol, 10 mL) using ultrasonic agitation for 2 min. DMAEMA monomer (30 mL, 5.0 g) was added into a mixture then the mixture was

degassed. A copper (I) bromide (0.5 mmol, 0.1 g) and bipyridyl (0.5 mmol, 0.33 g) were used as catalyst and ligand respectively. The sealed reaction was agitated by stirring at room temperature for 24 h followed by magnetic decantation. Finally, the precipitate was washed with water, ethanol, and hexane respectively [11, 52].

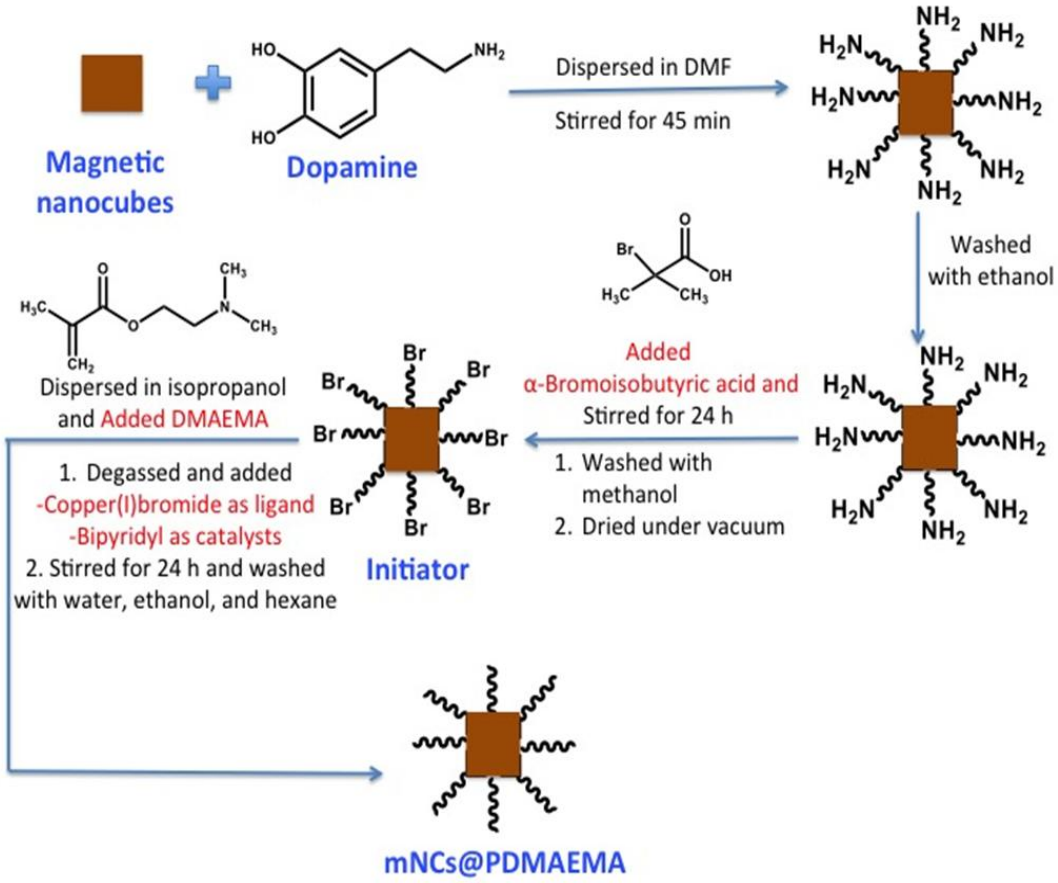

Figure3. 4 *A schematic presentation of synthesis of FMNCs/PDMAEMA using dopamine.*

3.5 Loading FMNCs/PDMAEMA with alkaline hypochlorite and *in vitro* drug release study.

To determine the magnetic nanocube as drug carrier as shown in **Figure 3.5**, the alkaline hypochlorite solution was in addition with stirring to 3 mL of FMNCs/PDMAEMA nanoparticles in distilled water (with the concentration of 2.5 mg/mL). The solution was continuously shaken overnight at room temperature in order to let the drug penetrate into the polymer layer. Moreover, the black FMNCs were magnetically

precipitated and consequently isolated by centrifugation. The calculation of drug loading capacity was estimated as follows

Loading capacity (%)

= 100 × (initial weight of drug – weight of free drug)/(initial weight of the FMNCs/PDMAEMA)

The drug-loaded magnetic nanocubes were brought into dialysis bag and dipped into 3 buffers (0.01M), including pH 5 cacodylate buffer, pH 7 phosphate buffer solution, and pH10 carbonate-bicarbonate at 37 ºC. With stirring in the dark, aliquots (4mL) of the buffer solutions were operated at different time periods and then detected by a UV-Vis spectrometer at 292 nm [53, 54]. The total volume by adding a 4 mL of buffer solution was kept constant. The drug concentration was identified using standard curves as the equation below [27, 55-57].

$$\text{Cumulative release (\%)} = 100\ W_t/W;$$

Where W_t is the drug-released weight of FMNCs/PDMAEMA in which time t and W is the whole weight of the drug-loaded polymer shell.

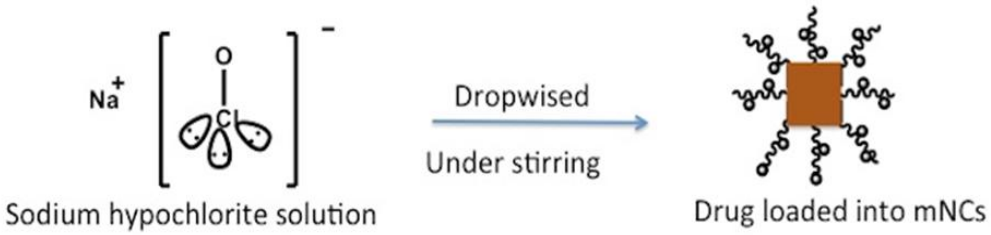

Figure3. 5 *Schematic representing the route of drug loading.*

3.6 Characterization of synthesized magnetic nanocubes coated with polymer.

The characteristic crystalline phases of magnetic nanoparticles and FMNCs were confirmed by using X-ray powder diffraction (XRD). X-ray powder diffraction (XRD) analyses were performed using Rigaku D/MaX-2200 Ultima-plus instrument with Cu K radiation (1.5418 A° source (40kV, 30mA). The powdered samples were placed on a glass holder. The scans were performed at 25°C in steps of 0.03° over 2-theta ranging from 20° to 70°.

The functionalities of polymer coating are confirmed by Fourier transform infrared (FT-IR) spectra that were recorded on an Impact 410 (Nicolet) spectrometer at frequencies ranging from 400 to 4000 cm^{-1}. Samples were thoroughly mixed with KBr and pressed into a pellet form.

The morphology of magnetic nanocubes, in the kind of size and shape analysis, was estimated by using Transmission electron microscopy (TEM) of FMNCs that was operated on a JEOL 2100CX (200 kV) microscope. Drops of the FMNCs solution in chloroform were dropped and evaporated at room temperature on a carbon-coated copper grid.

Scanning electron microscopy (SEM) was used to observe morphology of dentine discs. The pore sizes were observed under scanning electron microscope (JSM-5410 JEOL, Japan).

For a crystal-clear evidence of magnetic nanocube morphology, the confirmation of those was identified by Field emission scanning electron microscope (FE-SEM) that was performed on a JEOL JSM 7610 F instrument. Drops of the FMNCs solution in chloroform were dropped and evaporated at room temperature on a carbon-coated copper grid.

Thermogravimetric analysis (TGA) measurement, which was used to observe the weight loss of polymer coating, was performed on a Pyris 1 TGA (Perkin Elmer) instrument. All of specimens were evaporated in a vacuum oven at 60 °C prior to each measurement of TGA analysis for water and volatile solution removal. The 5 and 10 mg, which were tested for sample used, were heated from 20 to 850 °C at a heating rate of 25 °C min^{-1} under nitrogen atmosphere.

Inductively Coupled Plasma Optical Emission Spectrometry (ICP-OES) was used for determining quantity of Fe atom that is related to the amount of FMNCs in the composites. For determination of quantity of Fe, the dispersion of MNCs was digested with concentrated hydrochloric (HCl), and then the solution was filtrated with filters with 0.2 micrometers cut-off. After that the filtrates were measured by ICP-OES for analysis of quantity of Fe in the solution that pass through dentine disc

3.7 Cell culture.

The culture of L929 and raw264.7 cells (Fibroblast and macrophage cell lines) was performed in Dulbecco's modified Eagle's medium (DMEM) supplied with 10% FBS (fetal bovine serum) and 1% antibiotics at 37ºC incubated in a humidified atmosphere composed of 5% CO_2 atmosphere [30].

3.8 Cytotoxicity measurement.

L929 and raw264.7 cells were prepared to determine the cytotoxicity of the synthesized modified FMNCs. The FMNCs/PDMAEMA were dissolved with different concentration from 4 to 500 µg/mL of DMEM. L929 and raw264.7 cells were deposited into 96-well plates with ca. 30,000 cells/well in 200 µL medium with incubation of 24 h at 37 ºC. Then the culture was carefully abolished and filled with 200 µL of fresh medium comprising the serial concentration of FMNCs/PDMAEMA to incubate the cells. The MTT assays stock solution of 20 µL of 5 mg/mL in PBS was toted to each well after 48 h incubation at 37ºC and further incubated for 1.5 hours at 37ºC. Lastly, removing the medium containing unreacted dye and adding 200 µL per well DMSO to

fuse the achieved purple formazan crystals were performed. The absorbance was detected in a BioTek Elx80 Absorbance Reader at 490 nm [26].

3.9 Preparation of dentine disc

The preparation of dentine discs used in the study of dentine infiltration was performed without a consequence of a carious lesion resulting in a ready-to-use or an intact dentine. Firstly, 0.01 M phosphate buffered saline (PBS) was used to store the teeth at 4°C for and not more than 4 weeks. A cross section of dentine disc was prepared using a low speed round steel bur from carious teeth. Most importantly, the dentine thickness should not be less than 0.7 mm. in the part of the cavity floor and pulpal horn, and intact teeth were sliced as close as possible to the pulp chamber for sample utilization. Then, the dentine discs were neatly polished on an abrasive rotator. To remove smear layers, 35% of phosphoric acid was introduced for 10 s, and further rinsed with DI water for 5 min following with 10 min sonication.

3.10 Study of particles infiltration through dentine discs

For the estimation of infiltration through as-prepared dentine discs, the synthesized FMNCs were used to study. A concentration of 5 mg/mL FMNCs was employed in this study. The determining times as interval of sampling time were 0, 15, 30, 45, and 60 min for observing the release ratio of modified FMNCs. The quantity of Fe was measured by ICP technique at each determining time.

Thereby, the infiltration experiment set-up comprised of an injection tube, clamp, O-ring rubbers, and a permanent magnet. The apparatus as shown in **Figure 3.6** was set with the length of injection tube about 6.20 cm and tiny tube width of 0.5 cm in diameter. Magnetic strength from a rare-earth magnet is 32.59×10^2 gauss[41].

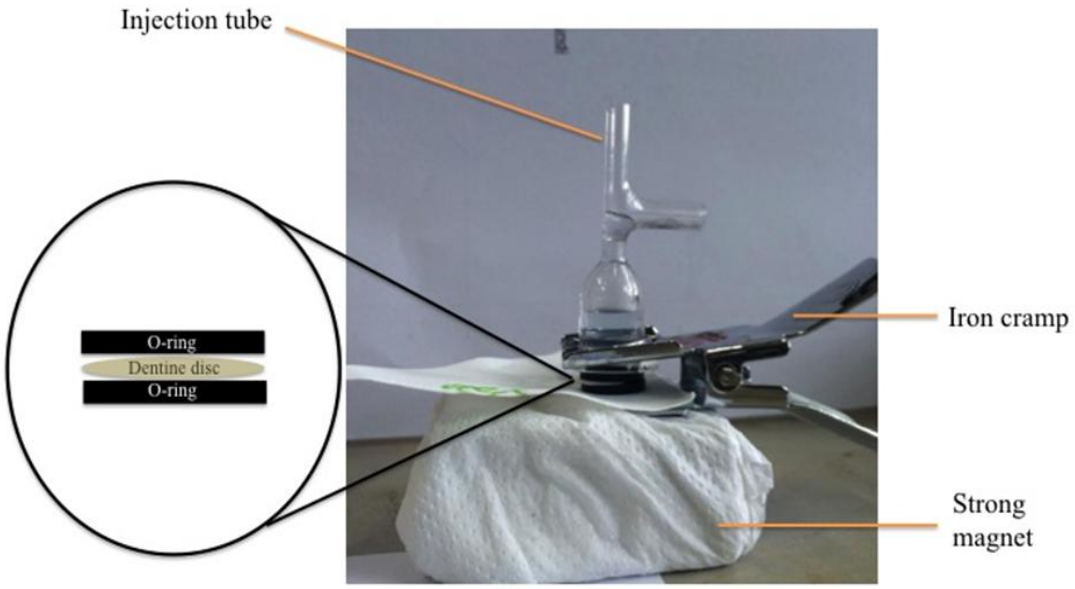

Figure3. 6 *Illustration of experiment setup for infiltration through the dentine disc, strong magnetic field (32.59 x 10^2 gauss).*

CHAPTER IV
RESULTS AND DISCUSSIONS

Herein, this part is mainly about the discussion criteria and results from experiments. For the first part in this work, the as-synthesized and PDMAEMA-modified FMNCs were characterized to identify the compositions, sizes and shapes. For the second part, the FMNCs infiltration through dentine disc, and drug release from the FMNCs were studied and characterized to investigate the potential for use in drug delivery system.

4.1 Characterization of synthesized FMNCs.

The method of themal decomposition has been investigated to be highly competent for magnetic iron oxide nanocubes preparation. The quantity of iron acetylacetonate, oleic acid, and benzyl ether were properly added to control the formation of nuclei. The high temperature of thermal decomposition yielded a regular shape and size for the magnetic iron oxide nanocubes with high crystallinity and comparatively monodisperse and well-controlled size distribution as it was presented by Woodward *et al* [58]. Typically, the metal complex variety (such as Fe $(acac)_3$) and surfactants (such as oleic acid and oleylamine) in organic solvents that is not easy to volatile (such as phenyl ether) were basically required in the thermal decomposition method. Structural information from magnetic FMNCs was derived from both of TEM and XRD.

As an effectively repeated result for determining the ratio of solvent and time used for the optimized condition, the TEM images as shown in **Figure 4.1** could be explained and identified that the ratio of solvent and time used had an impinge on FMNCs sizes due to differences in nucleation and growth. According to various sizes of FMNCs obtained, less benzyl ether in the solution resulted in the bigger particle size. Moreover, reaction time is crucially dependent with decomposition and oxidation of iron oxide formation. As a consequence of determining the reaction time, the greater time helped to complete iron oxide formation at the oxidation step. To succeed 60-

nm-size FMNCs, the 1:0.75 ration of iron acetylacetonate and benzyl ether ratio was determined as the optimum condition, and suitable reaction time was performed at an hour.

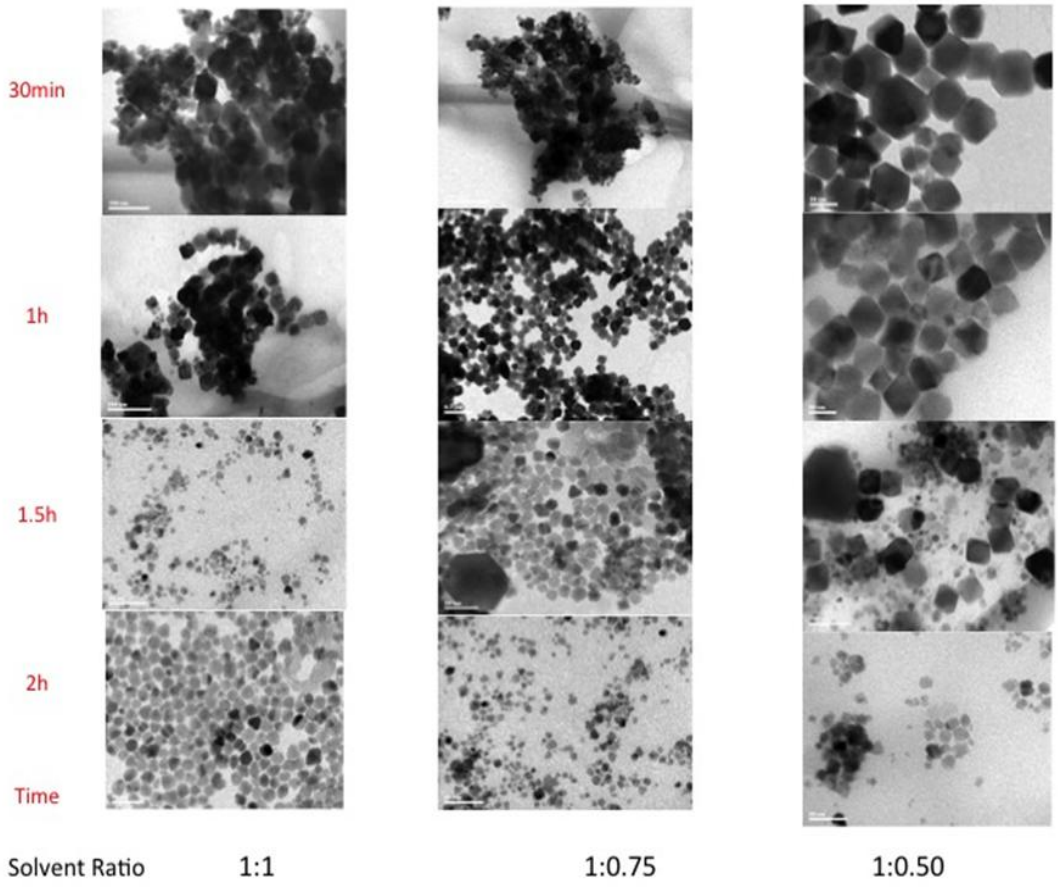

Figure4. 1 *TEM images of synthesized FMNCs by varying ratio of solvent and time used.*

For the optimum condition used in this work, FMNCs was confirmed by following techniques. For **Figure 4.1**, the TEM image of as-synthesized iron oxide nanocubes exhibited a well-defined cubic form with a ca. 60 nm in diameter size average from statistical analysis of TEM images, showing high monodispersity of MNCs. Likewise, the FE-SEM image also confirmed the uniform cubic-shaped structure of MNCs as shown in **Figure 4.2**. The position and intensity of all diffraction peaks from XRD patterns are

consistent with those of the standard Fe_3O_4 magnetic powder shown as shown in **Figure 4.3**.

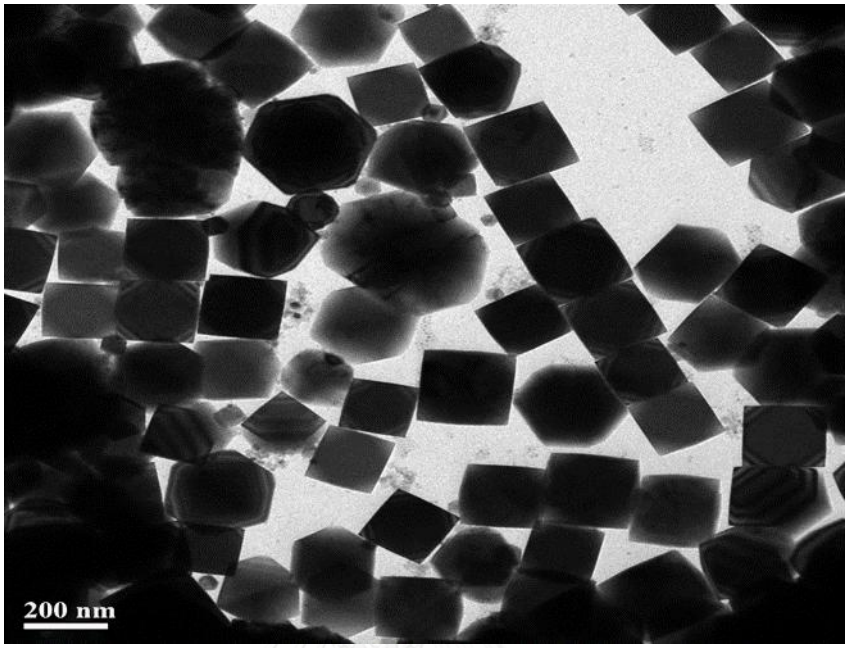

A

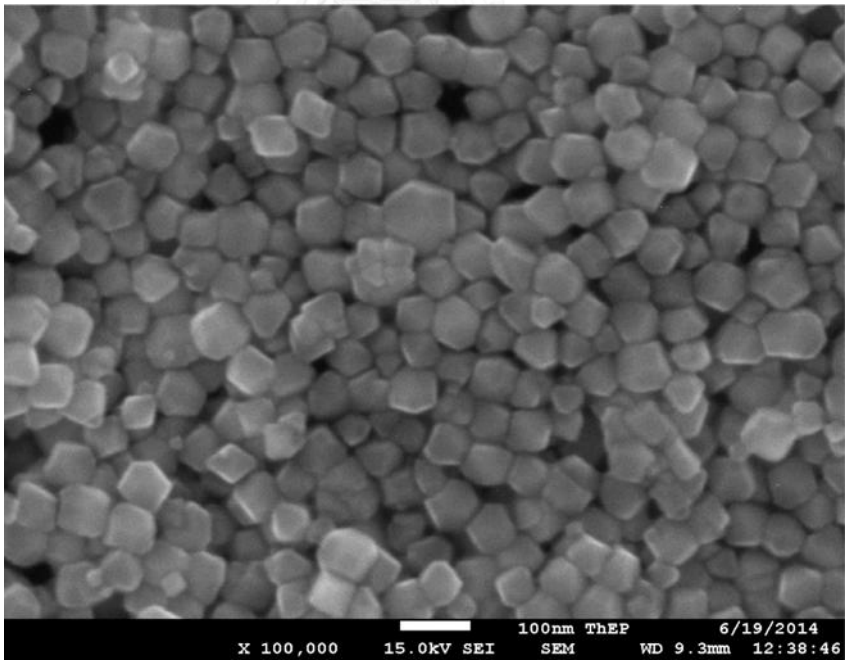

B

Figure4. 2 *TEM image (A) of FMNCs and FE-SEM image (B) of FMNCs.*

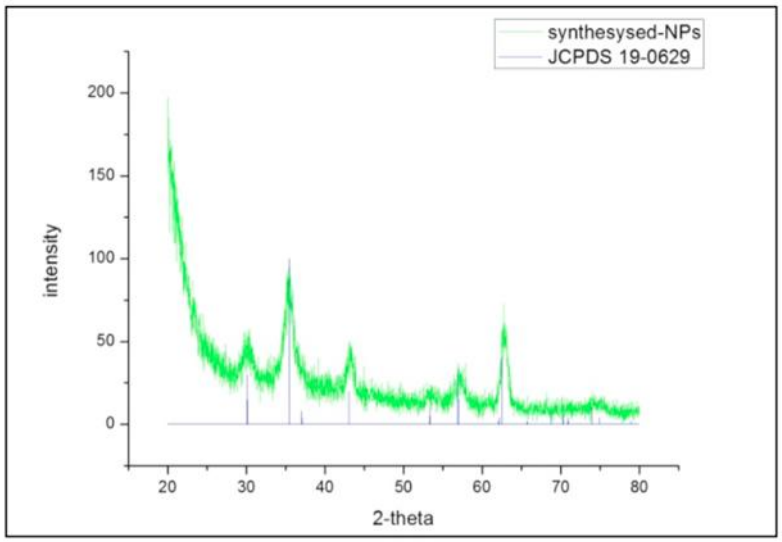

Figure4. 3 *XRD pattern of the synthesized magnetite nanocubes comparing with the standard pattern of Fe_3O_4 (file JCPDS 19- 0629).*

4.2 Preparation of PDMAEMA-modified magnetic iron oxide nanocubes.

For synthesis of FMNCs/PDMAEMA optimization, all of the four varied conditions were successfully accomplished. The morphology and size of FMNCs/PDMAEMA were characterized by TEM and FTIR techniques. For the ease in preparation, which used the simple method (no reflux) for forming an initiator and polymerization by ATRP at mild condition, and the quality of products, the Route 4 was indicated the best condition as observed from all of the TEM images, as depicted in **Figure 4.4**. The TEM image of the composites from Route 4 could be observed a thickest cloud elucidated as PDMAEMA coating with dispersed and homogeneous size particles. Besides, FTIR spectrum as shown in **Figure 4.5** could identify the successful PDMAEMA coating onto FMNCs since there was the presence of indicative bands such as methylene, methyl vibration between 2980-2800 cm^{-1}, and absorption bands at around 1700 cm^{-1} for the ester group stretching (C=O) from PDMAEMA components [1]. As a result of the four varied condition, the characteristic absorption at 2980 cm^{-1} in Route 1 was lower

intensity meaning that PDMAEMA coating in Route 1 may not be thick or a little amount of polymer cloud comparing to the others.

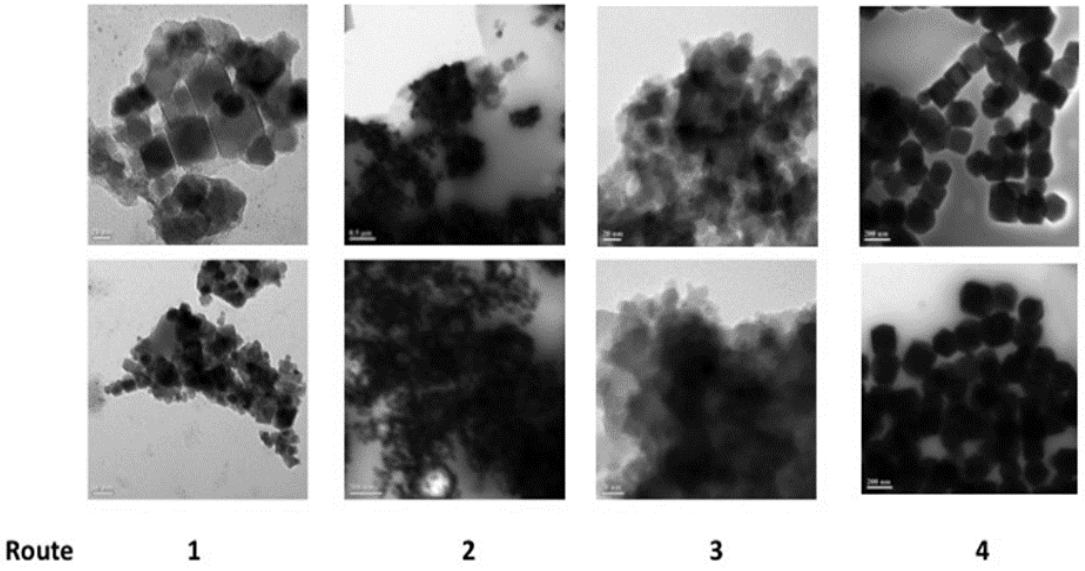

Figure4. 4 *TEM images of FMNCs coated with PDMAEMA in all of routes with various conditions.*

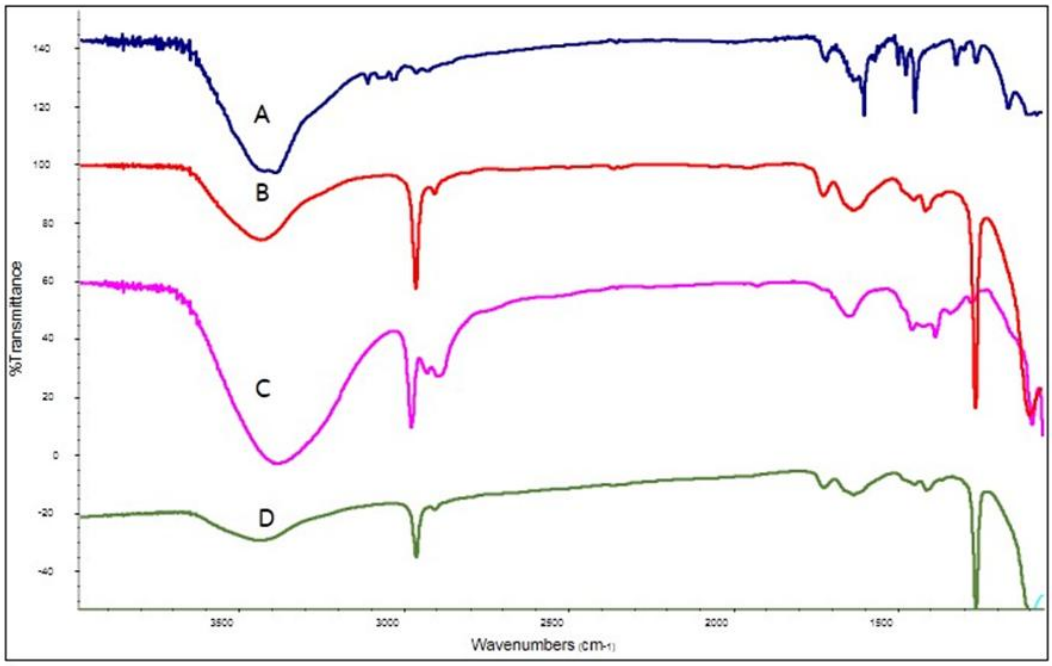

Figure4. 5 *FTIR spectrum of FMNCs coated with PDMAEMA in all of routes with various conditions; (a) Route 1, (b) Route 2, (c) Route 3, (d) Route 4.*

For a stronger interaction between an initiator and iron oxide particles and thicker polymer coating owing to high loading capacity, dopamine was; however, used to further attach more hydroxyl groups. Such a surface modification resulted in the particles with thicker polymer coating on their surface as confirmed by TEM technique in **Figure 4.6**. Accordingly, TEM images confirmed the thicker PDMAEMA coating onto FMNCs surface.

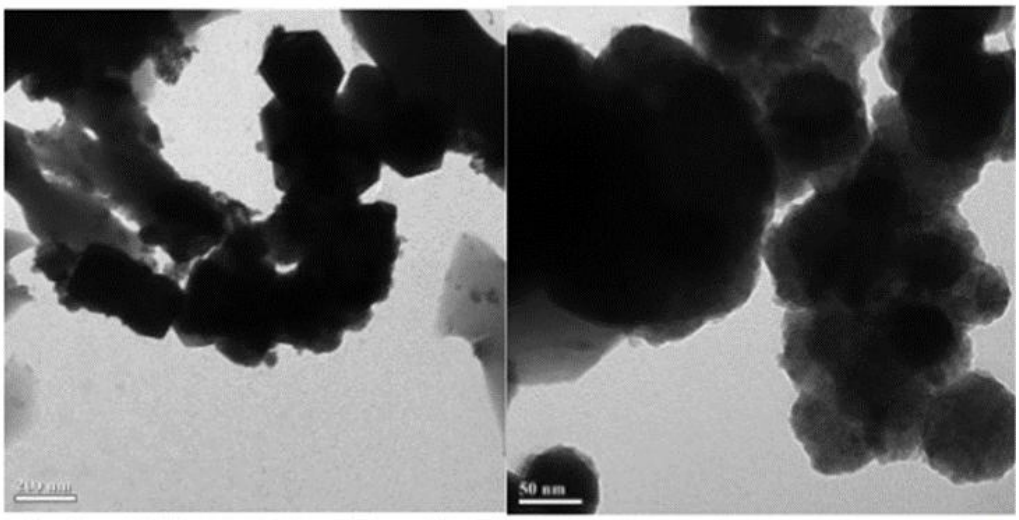

Figure4. 6 *TEM images of FMNCs/PDMAEMA with dopamine applied.*

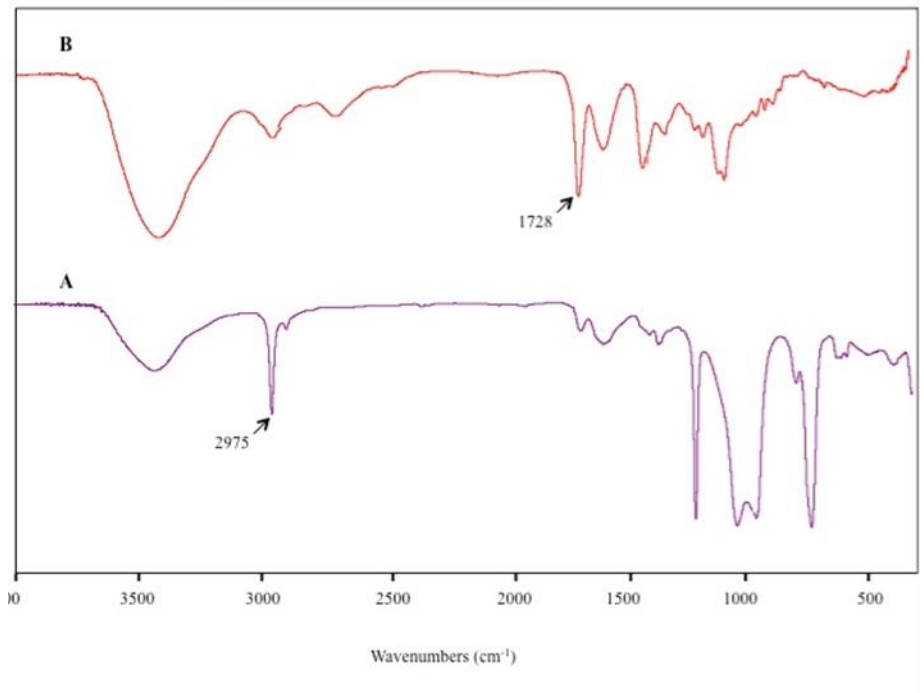

Figure4. 7 *FT-IR spectra of (A) FMNCs and (b) FMNCs/PDMAEMA.*

Moreover, the thicker and indistinct FMNCs/PDMAEMA were confirmed by both FT-IR and TGA measurements. For confirmation of polymer coating by using dopamine, FT-IR spectrum exhibited the stronger peak at 2975 cm^{-1} for methyl groups in OA and absorption band of the (CO)–O–H group at 1292 cm^{-1}, contributed to the chemisorption of -COOH to the FMNCs, and a higher intensity of characteristic absorption band at 1728 cm^{-1} corresponding to the ester group stretching (C=O) from a part of PDMAEMA was crystal-clear seen in the FT-IR spectrum as shown in **Figure 4.7**. The TGA curves as shown in **Figure 4.8** exhibit about weight loss of FMNCs and composites. The TGA curve of unmodified FMNCs (red) showed little weight loss attributed to decomposition of the initiator modified onto FMNCs surface. Moreover, the TGA curve of FMNCs/PDMAEMA could identify the weight loss about 4%.

On the contrary, as observed in the FMNCs/PDMAEMA with dopamine applied, the TGA curves showed obviously a single-stage weight loss upon heating under nitrogen. The stage accounts for polymer degradation for about 8.75% of the weight loss, which is higher than that of FMNCs/PDMAEMA, in the run of 380 – 700 ºC, informing the PDMAEMA attribution [1].

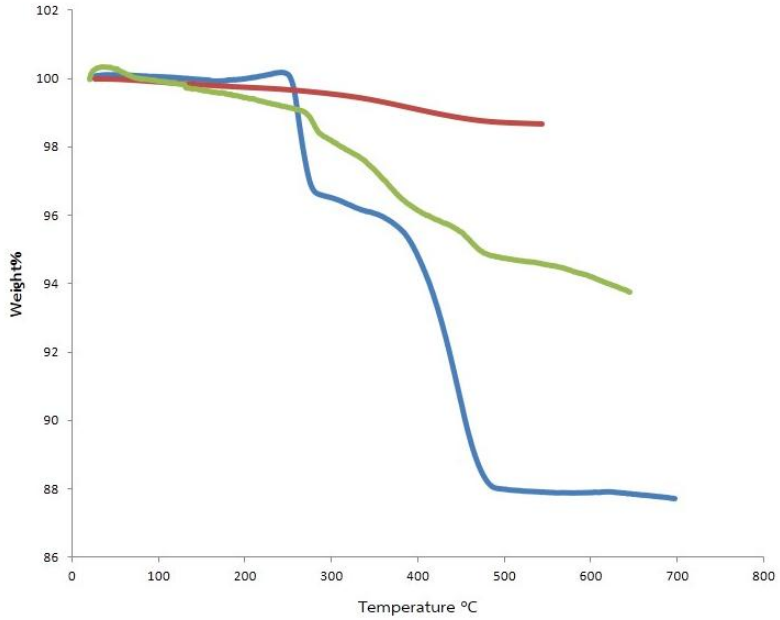

Figure4. 8 *TGA curves of FMNCs (red), FMNCs/PDMAEMA (green), and FMNCs/PDMAEMA with dopamine applied (blue).*

4.3 Dentin preparation and infiltration of FMNCs/PDMAEMA.

As well-prepared dentine discs by a formerly stated method, the morphology of dentine disc surface and before-and-after dentine infiltration were particularly explored and observed by SEM technique as shown in **Figure 4.9**. It could be observed that surface and tubules of dentine disc in **Figure 4.9A** and B could confirm the achieved clean surface and tubules. In addition, inductively coupled plasma atomic absorption spectroscopy (ICP-AAS) was used to investigate the amount of FMNCs/PDMAEMA during the time as shown in **Figure 4.10.** Apparently, it was significantly noticed that FMNCs/PDMAEMA could infiltrate almost 20% of all through the dentine disc only in 30 min and about 70% for an hour as demonstrated in Figure 4.11. From the observation of dentin infiltration of FMNCs/PDMAEMA, it was obviously that they could be infiltrated and penetrated by an external magnet as a consequence of black magnetic spot on the filter paper and confirmed SEM images of successful FMNCs/PDMAEMA loading in **Figure 4.9 C and D**.

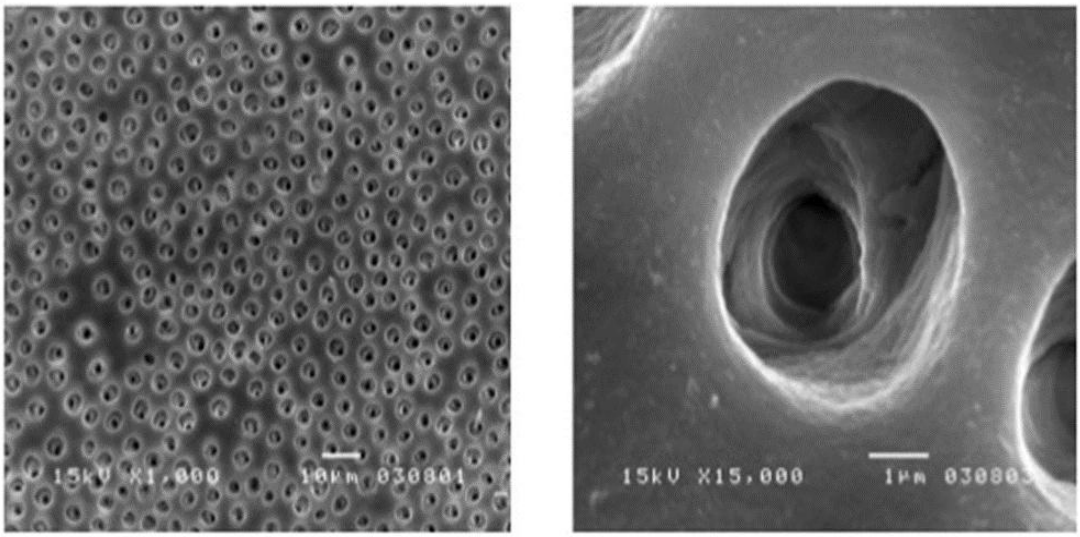

A B

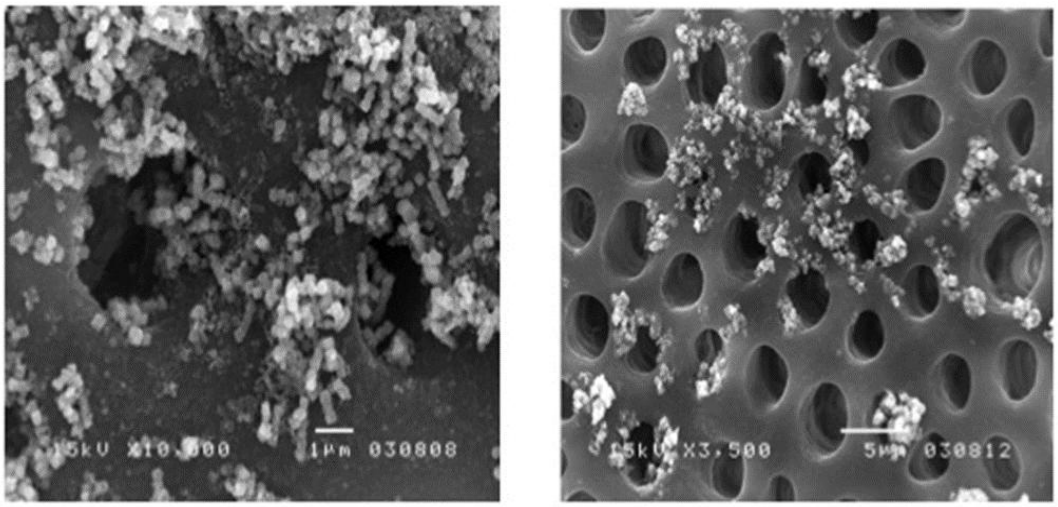

Figure4. 9 *Dentine preparation and infiltration of (a) surface of a clean dentine disc, (b) a zoom-in dentinal tubule, (c) and (d) front and back of FMNCs/PDMAEMA infiltrated through dentin disc*

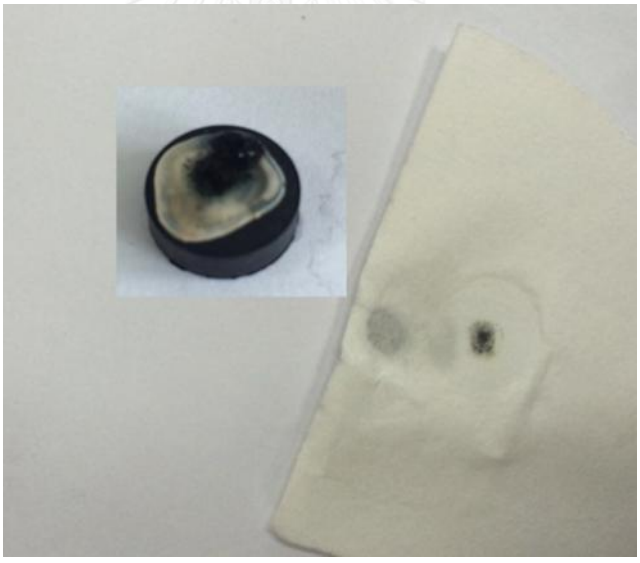

Figure4. 10*. Dentine infiltration of FMNCs/PDMAEMA on a filter paper.*

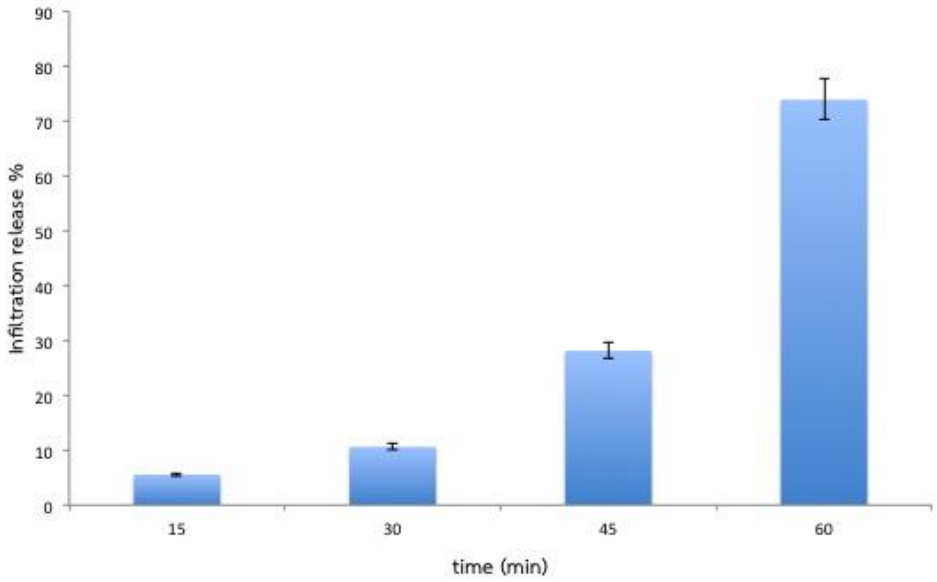

Figure4. 11 Dentine infiltration profile of FMNCs/PDMAEMA.

4.4 Drug release study and cytotoxicity measurement.

As study of biomedical applications, it is crucial to estimate the efficacy of toxicity of the FMNCs/PDMAEMA. Here, the *in vitro* cytotoxicity of FMNCs/PDMAEMA with various administered concentrated solutions varying from 4 to 500 μg/mL against L929 and Raw264.7 cells was estimated through MTT assay. As shown in **Figure 4.12**, the cell viability of FMNCs/PDMAEMA, in which48 h incubation was performed, below 500 μg/mL remains mostly existed considered with the untreated cells, implying a low cytotoxicity of the FMNCs/PDMAEMA.

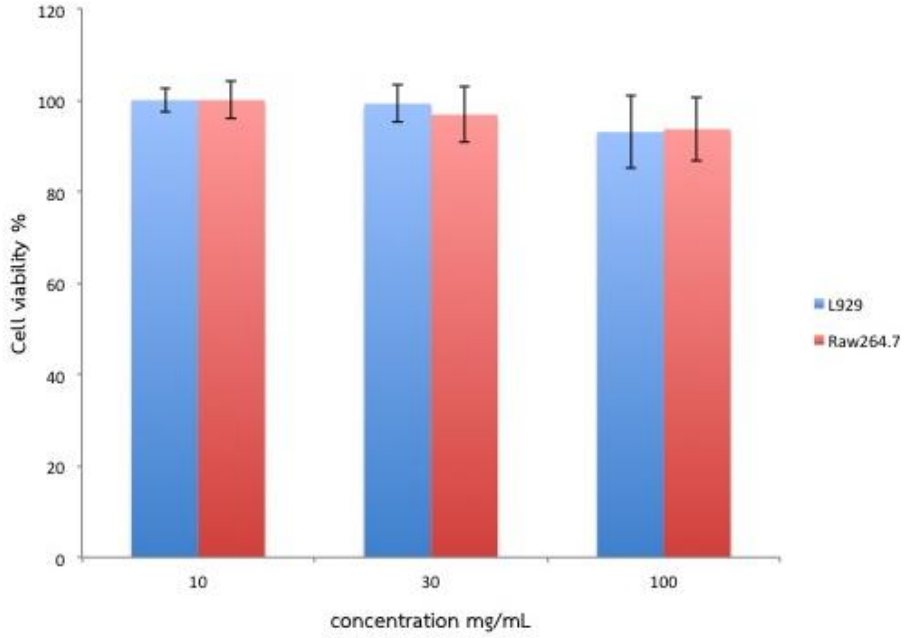

Figure4. 12 Cytotoxicity of FMNCs/PDMAEMA against L929 and Raw264.7 cells.

In *in vitro* pH-sensitive behavior of drug release for evaluating FMNCs/PDMAEMA efficacy as a drug carrier materials, alkaline hypochlorite, which is used as a disinfectant or a bleaching agent, was entrapped into FMNCs/PDMAEMA, and the alkaline hypochlorite let-off test in pH 5, 7, and 10 in various buffer solutions was operated at 37 °C. After free alkaline hypochlorite elimination, the capacity of the drug-loaded FMNCs/PDMAEMA as in the previous method is 6.02%, which is quite high in a comparison with the formerly noted drug loading capacity (～2.03%) of the PEG-modified FMNCs [9]. It could be explained that the modified FMNCs in this work exploit the denser polymer shells, which benefits in developing ion-dipole interaction and hydrogen bonding with alkaline hypochlorite resulting in improvement in the loading capacity. The cumulative release amounts of alkaline hypochlorite from the FMNCs/PDMAEMA within 48 h at pH 5, 7, and 10 are 97.67%, 86.00%, and 23.55%, respectively as shown in Figure 4.13. The cumulative release amount was clearly eminent at pH 5 and 7 than that at pH 10. An accessible explanation was that PDMAEMA chains and alkaline hypochlorite were protonated at pH 5 since PDMAEMA

and hypochlorite exhibit pKa values of 7.5 and 7.53, respectively. The ion-dipole interaction between PDMAEMA and alkaline hypochlorite may be diminished, and are able to sparingly released.

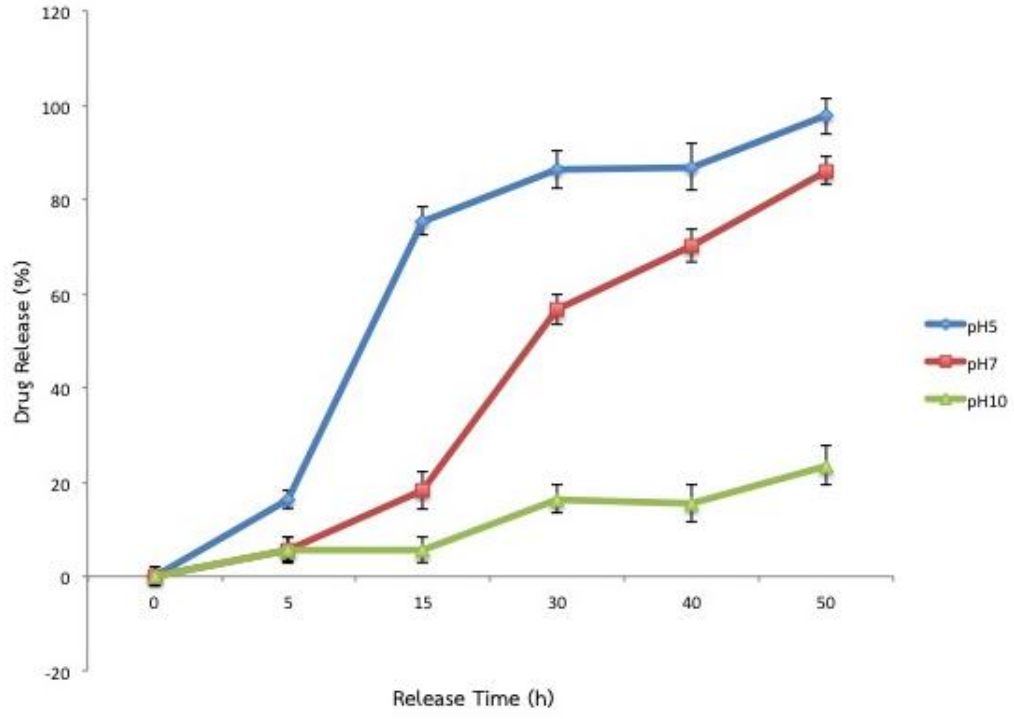

Figure4. 13 *Drug release profiles from alkaline hypochlorite-loaded FMNCs/PDMAEMA.*

CHAPTER V
CONCLUSION

Successfully, the thermal decomposition by using iron acetylacetonate as starting materials, oleic acid as surfactant, and benzyl ether as excellent solvent was used to synthesize uniformed FMNCs by varying a ratio content of solvent which it was best performed at 75% benzyl ether. As a result of synthesized FMNCs, the desired size FMNCs could be practically obtained with 60-nm in diameter of which optimum condition at 290°C with rate 20°C/min defined as repeatable synthesized FMNCs in this work.

A copper-mediated ATRP was accomplishedly varied and carried out to prepare the PDMAEMA-modified FMNCs with good biocompatibility and well-dispersed nanocubes. According to synthesis optimization, the use of α-bromoisobutyric acid as an initiator and bipyridyl as ligand helped in the successful polymerization. Moreover, dopamine was introduced to be an extra hydroxyl group onto FMNCs surface for enhancing the interaction with the initiator resulting in thicker PDMAEMA coating with higher drug loading capacity.

As dentine infiltration demonstrated and explored, the preparation of dentine disc with 35% of phosphoric acid was effectively done as a result of clear dentine discs. For observation of dentine infiltration, FMNCs/PDMAEMA could be infiltrated and penetrated induced by external magnet through dentine discs as confirmed by SEM images.

In addition, alkaline hypochlorite as an antiinfective drug model was loaded into the PDMAEMA shell of the modified FMNCs, and consequently, drug release was exploited in buffer solution (pH 5, 7, and 10) at 37 °C. The results verified that PDMAEMA-modified nanocubes as a drug carrier exhibit pH-sensitive drug release behavior. Moreover, MTT assay of alkaline hypochlorite-loaded PDMAEMA modified FMNCs against L929 and Raw264.7 cells further confirmed that the FMNCs/PDMAEMA could be utilized for enhancing the controllable drug delivery. Hence, the

FMNCs/PDMAEMA with novel structures and magnificent properties have been completely prepared, which is a huge advantage to further optimize potential biomedical applications of magnetic materials as drug carriers.

In summary, this work can discover newly drug delivery system by using FMNCs/PDMAEMA through dentine discs. This system is another alternative clinical way for an improvement and development in the future. Since the magnetic carrier property easily helps in drug delivery system, it can be further applied in the fact that it does not face a high risk of its application and a complex for dentistry practices. Eventually, it needs more improvement and development to be done to increase the delivery efficiency and develop effective applications.

REFERENCES

1. He, X., et al., *Functionalization of magnetic nanoparticles with dendritic-linear-brush-like triblock copolymers and their drug release properties.* Langmuir, 2012. **28**(32): p. 11929-38.
2. Wu, W., Q. He, and C. Jiang, *Magnetic iron oxide nanoparticles: synthesis and surface functionalization strategies.* Nanoscale Res Lett, 2008. **3**(11): p. 397-415.
3. Akbarzadeh, A., M. Samiei, and S. Davaran, *Magnetic nanoparticles: preparation, physical properties, and applications in biomedicine.* Nanoscale Res Lett, 2012. **7**(1): p. 144.
4. Kalia, S., et al., *Magnetic polymer nanocomposites for environmental and biomedical applications.* Colloid and Polymer Science, 2014. **292**(9): p. 2025-2052.
5. Subhankar Bedanta, O.P.a.W.K., *Handbook of Magnetic Materials.* Elsevier, 2015. **23**: p. 1-83.
6. Mahmoudi, M., et al., *Superparamagnetic iron oxide nanoparticles (SPIONs): development, surface modification and applications in chemotherapy.* Adv Drug Deliv Rev, 2011. **63**(1-2): p. 24-46.
7. Noh, S.H., et al., *Nanoscale magnetism control via surface and exchange anisotropy for optimized ferrimagnetic hysteresis.* Nano Lett, 2012. **12**(7): p. 3716-21.
8. Bhandari, R., et al., *Single step synthesis, characterization and applications of curcumin functionalized iron oxide magnetic nanoparticles.* Materials Science and Engineering: C, 2016. **67**: p. 59-64.
9. Du, P., et al., *Biocompatible magnetic and molecular dual-targeting polyelectrolyte hybrid hollow microspheres for controlled drug release.* Mol Pharm, 2013. **10**(5): p. 1705-15.
10. O'Brien, F.J., *Biomaterials & scaffolds for tissue engineering.* Materials Today, 2011. **14**(3): p. 88-95.

11. Akbarzadeh, A., et al., *Synthesis, characterization, and in vitro evaluation of novel polymer-coated magnetic nanoparticles for controlled delivery of doxorubicin.* Nanotechnol Sci Appl, 2012. **5**: p. 13-25.
12. Mahanani, E.S., *Essential of Oral Histology and Embriology.* Mosby, 2000.
13. Balaev, D.A., et al., *Magnetic properties of heat treated bacterial ferrihydrite nanoparticles.* Journal of Magnetism and Magnetic Materials, 2016. **410**: p. 171-180.
14. Krumina, L., et al., *Desorption mechanisms of phosphate from ferrihydrite and goethite surfaces.* Chemical Geology, 2016. **427**: p. 54-64.
15. Yu, S., C.-J. Sun, and G.-M. Chow, *1 - Chemical Synthesis of Nanostructured Particles and Films A2 - Koch, Carl C*, in *Nanostructured Materials (Second Edition)*. 2007, William Andrew Publishing: Norwich, NY. p. 3-46.
16. Atabaev, T.S., *Chapter 8 - Multimodal inorganic nanoparticles for biomedical applications A2 - Grumezescu, Alexandru Mihai*, in *Nanobiomaterials in Medical Imaging*. 2016, William Andrew Publishing. p. 253-278.
17. Karimzadeh, I., et al., *A novel method for preparation of bare and poly(vinylpyrrolidone) coated superparamagnetic iron oxide nanoparticles for biomedical applications.* Materials Letters, 2016. **179**: p. 5-8.
18. Karimzadeh, I., H.R. Dizaji, and M. Aghazadeh, *Development of a facile and effective electrochemical strategy for preparation of iron oxides (Fe3O4 and γ-Fe2O3) nanoparticles from aqueous and ethanol mediums and in situ PVC coating of Fe3O4 superparamagnetic nanoparticles for biomedical applications.* Journal of Magnetism and Magnetic Materials, 2016. **416**: p. 81-88.
19. Munjal, S., et al., *Water dispersible CoFe2O4 nanoparticles with improved colloidal stability for biomedical applications.* Journal of Magnetism and Magnetic Materials, 2016. **404**: p. 166-169.
20. Qiao, L. and M.T. Swihart, *Solution-Phase Synthesis of Transition Metal Oxide Nanocrystals: Morphologies, Formulae, and Mechanisms.* Advances in Colloid and Interface Science.

21. Ran, J., et al., *Atom transfer radical polymerization (ATRP): A versatile and forceful tool for functional membranes.* Progress in Polymer Science, 2014. **39**(1): p. 124-144.
22. Dong, H., et al., *Recyclable antibacterial magnetic nanoparticles grafted with quaternized poly(2-(dimethylamino)ethyl methacrylate) brushes.* Biomacromolecules, 2011. **12**(4): p. 1305-11.
23. Freiberg, S. and X.X. Zhu, *Polymer microspheres for controlled drug release.* Int J Pharm, 2004. **282**(1-2): p. 1-18.
24. Karppi, J., et al., *Adsorption of drugs onto a pH responsive poly(N,N-dimethyl aminoethyl methacrylate) grafted anion-exchange membrane in vitro.* Int J Pharm, 2007. **338**(1-2): p. 7-14.
25. Lao, L.L., et al., *Modeling of drug release from bulk-degrading polymers.* Int J Pharm, 2011. **418**(1): p. 28-41.
26. Alépée, N., et al., *Assessment of cosmetic ingredients in the in vitro reconstructed human epidermis test method EpiSkin™ using HPLC/UPLC-spectrophotometry in the MTT-reduction assay.* Toxicology in Vitro, 2016. **33**: p. 105-117.
27. Sadri, A., V. Changizi, and N. Eivazadeh, *Evaluation of glioblastoma (U87) treatment with ZnO nanoparticle and X-ray in spheroid culture model using MTT assay.* Radiation Physics and Chemistry, 2015. **115**: p. 17-21.
28. Stepanenko, A.A. and V.V. Dmitrenko, *Pitfalls of the MTT assay: Direct and off-target effects of inhibitors can result in over/underestimation of cell viability.* Gene, 2015. **574**(2): p. 193-203.
29. Yang, Y., et al., *Evidence of ATP assay as an appropriate alternative of MTT assay for cytotoxicity of secondary effluents from WWTPs.* Ecotoxicology and Environmental Safety, 2015. **122**: p. 490-496.
30. He, W. and M.C. Frost, *CellNO trap: Novel device for quantitative, real-time, direct measurement of nitric oxide from cultured RAW 267.4 macrophages.* Redox Biology, 2016. **8**: p. 383-397.

31. Kurosawa, M., et al., *Streptococcus pyogenes CAMP factor attenuates phagocytic activity of RAW 264.7 cells.* Microbes and Infection, 2016. **18**(2): p. 118-127.
32. Chen, L., et al., *Functional magnetic nanoparticle/clay mineral nanocomposites: preparation, magnetism and versatile applications.* Applied Clay Science, 2016. **127–128**: p. 143-163.
33. Shaalan, M., et al., *Recent progress in applications of nanoparticles in fish medicine: A review.* Nanomedicine: Nanotechnology, Biology and Medicine, 2016. **12**(3): p. 701-710.
34. Trapiella-Alfonso, L., et al., *Electromigration separation methodologies for the characterization of nanoparticles and the evaluation of their behaviour in biological systems.* TrAC Trends in Analytical Chemistry.
35. Zarschler, K., et al., *Ultrasmall inorganic nanoparticles: State-of-the-art and perspectives for biomedical applications.* Nanomedicine: Nanotechnology, Biology and Medicine, 2016. **12**(6): p. 1663-1701.
36. Trindade, T. and P.J. Thomas, *4.13 - Defining and Using Very Small Crystals A2 - Reedijk, Jan*, in *Comprehensive Inorganic Chemistry II (Second Edition)*, K. Poeppelmeier, Editor. 2013, Elsevier: Amsterdam. p. 343-369.
37. Wu, Y., et al., *A Novel Approach to Molecular Recognition Surface of Magnetic Nanoparticles Based on Host-Guest Effect.* Nanoscale Res Lett, 2009. **4**(7): p. 738-747.
38. Zhao, C., et al., *Polymeric pH-sensitive membranes—A review.* Progress in Polymer Science, 2011. **36**(11): p. 1499-1520.
39. Chen, Y.-H., et al., *Characterization of magnetic poly(methyl methacrylate) microspheres prepared by the modified suspension polymerization.* Journal of Applied Polymer Science, 2008. **108**(1): p. 583-590.
40. Hu, F.X., K.G. Neoh, and E.T. Kang, *Synthesis and in vitro anti-cancer evaluation of tamoxifen-loaded magnetite/PLLA composite nanoparticles.* Biomaterials, 2006. **27**(33): p. 5725-33.

41. Besinis, A., R. van Noort, and N. Martin, *Infiltration of demineralized dentin with silica and hydroxyapatite nanoparticles.* Dental Materials, 2012. **28**(9): p. 1012-1023.

42. Besinis, A., R. van Noort, and N. Martin, *The use of acetone to enhance the infiltration of HA nanoparticles into a demineralized dentin collagen matrix.* Dental Materials, 2016. **32**(3): p. 385-393.

43. Jee, S.E., et al., *Investigation of ethanol infiltration into demineralized dentin collagen fibrils using molecular dynamics simulations.* Acta Biomaterialia, 2016. **36**: p. 175-185.

44. Hass, V., et al., *Collagen cross-linkers on dentin bonding: Stability of the adhesive interfaces, degree of conversion of the adhesive, cytotoxicity and in situ MMP inhibition.* Dental Materials, 2016. **32**(6): p. 732-741.

45. Hass, V., et al., *Degradation of dentin-bonded interfaces treated with collagen cross-linking agents in a cariogenic oral environment: An in situ study.* Journal of Dentistry, 2016. **49**: p. 60-67.

46. Iqbal, K., et al., *Effect of High-Intensity Focused Ultrasound on Enterococcus Faecalis Planktonic Suspensions and Biofilms.* Ultrasound in Medicine & Biology, 2013. **39**(5): p. 825-833.

47. Shrestha, A., et al., *Delivery of Antibacterial Nanoparticles into Dentinal Tubules Using High-intensity Focused Ultrasound.* Journal of Endodontics, 2009. **35**(7): p. 1028-1033.

48. Zhang, L., R. He, and H.-C. Gu, *Oleic acid coating on the monodisperse magnetite nanoparticles.* Applied Surface Science, 2006. **253**(5): p. 2611-2617.

49. Dokyoon Kim, N.L., Mihyun Park, Byung Hyo Kim, Kwangjin An, and Taeghwan Hyeon, *Synthesis of Uniform Ferrimagnetic Magnetite Nanocubes.* JACS, 2009. **131**: p. 454–455.

50. Robert T. Woodward, C.I.O., Erol A. Hassan, Humphrey H. P. Yiu, Matthew J. Rosseinsky, Jonathan V. M. Weaver, *Multi-Responsive Polymer-Stabilized Magnetic Engineered Emulsions as Liquid-Based Switchable Magneto-responsive Actuators.* The Royal Society of Chemistry, 2011. **48**: p. 2131.

51. Yuan, W., et al., *Synthesis, characterization, and controllable drug release of dendritic star-block copolymer by ring-opening polymerization and atom transfer radical polymerization.* Polymer, 2007. **48**(9): p. 2585-2594.

52. Marcelo, G., A. Muñoz-Bonilla, and M. Fernández-García, *Magnetite–Polypeptide Hybrid Materials Decorated with Gold Nanoparticles: Study of Their Catalytic Activity in 4-Nitrophenol Reduction.* The Journal of Physical Chemistry C, 2012. **116**(46): p. 24717-24725.

53. Gordon, S., *Dichloropropanone Lab.* Canadian Journal of Chemistry, 1986. **64**: p. 1250-1266.

54. Patricia Paviet-Hartmann1, J.D., Thomas Hartmann1, Stanislaw Marczak1, and M.W. Ningping Lu1, Andrzej Rafalski3, Zbigniew Zagorski3, *SPECTROSCOPIC INVESTIGATION OF THE*

FORMATION OF RADIOLYSIS

BY-PRODUCTS BY 13/9 MeV LINEAR

ACCELERATOR OF ELECTRONS (LAE) IN SALT. 3The Institute of Nuclear Chemistry and Technology, 2002.

55. Long, Y., et al., *Highly selective, sensitive and naked-eye fluorescence probes for the direct detection of hypochlorite anion and their application in biological environments.* Sensors and Actuators B: Chemical, 2016. **232**: p. 327-335.

56. Ma, J., et al., *The effects of sodium hypochlorite and chlorhexidine irrigants on the antibacterial activities of alkaline media against Enterococcus faecalis.* Archives of Oral Biology, 2015. **60**(7): p. 1075-1081.

57. Ujihara, R., et al., *Effects of the ionic strength of sodium hypochlorite solution on membrane cleaning.* Journal of Membrane Science.

58. Shouheng Sun, † Hao Zeng,† David B. Robinson,† Simone Raoux,‡ Philip M. Rice,‡ and a.G.L. Shan X. Wang, *Monodisperse MFe2O4 (M) Fe, Co, Mn) Nanoparticles.* American Chemical Society, 2004. **126**: p. 273-279.

APPENDIX

Figure A 1 FMNCs solution (Left) and FMNCs/PDMAEMA solution (Right)

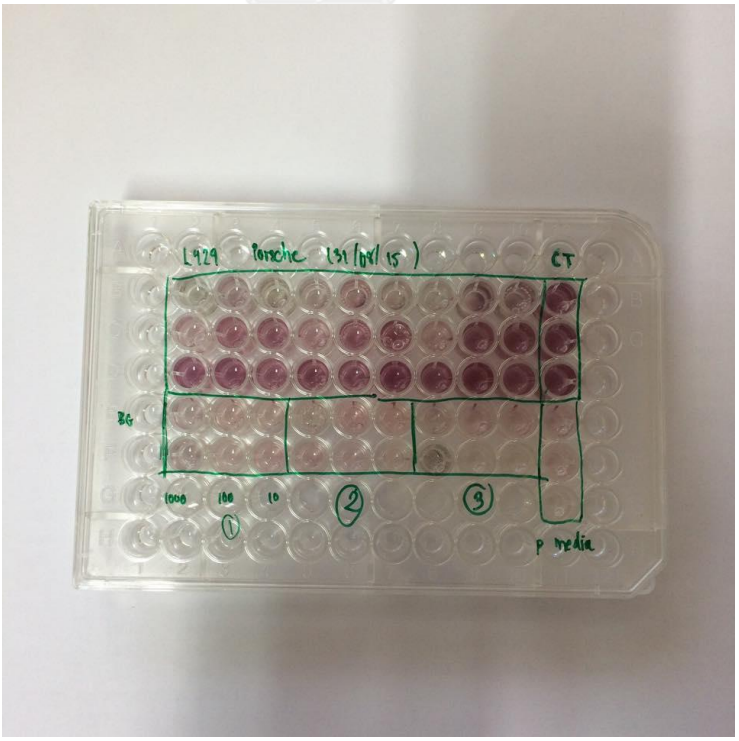

Figure A 2 Cytotoxicity study of FMNCs/PDMAEMA by using MTT assay

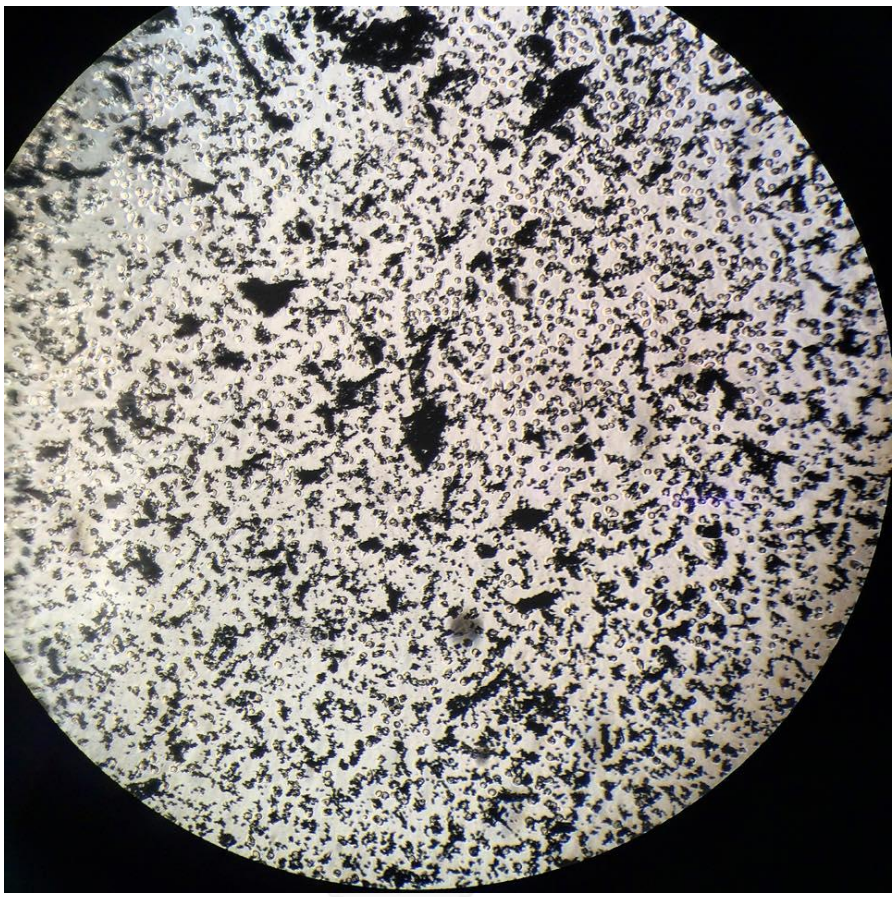

Figure A 3 FMNCs/PDMAEMA incubated with cells in cytotoxicity measurement.

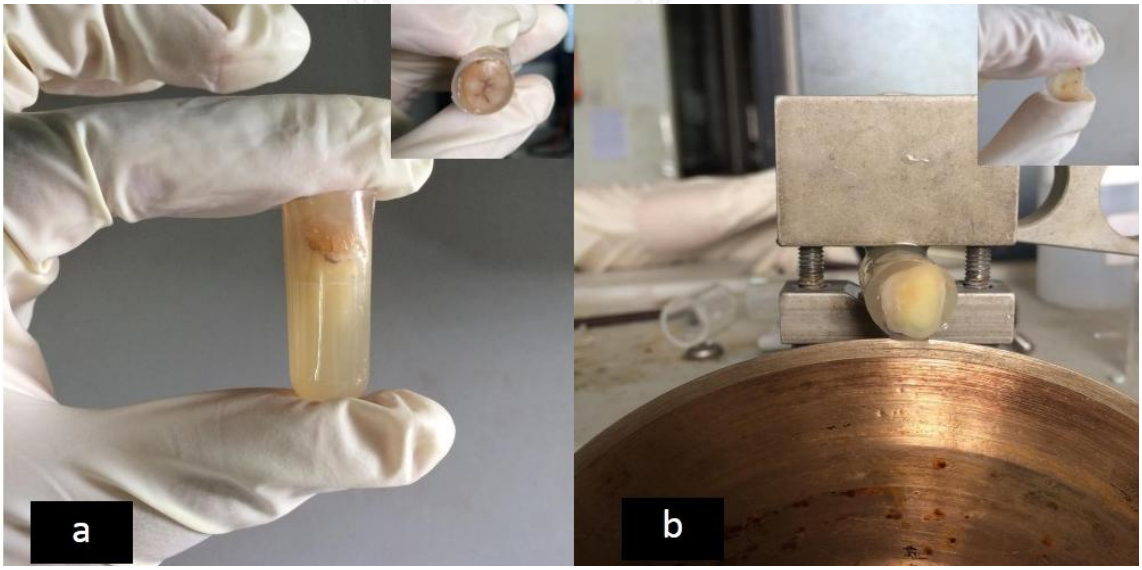

Figure A 4 Photographs of the preparation process of the dentine discs, (a) The dentine disc casting in a resin and (b) the dentine disc cutting

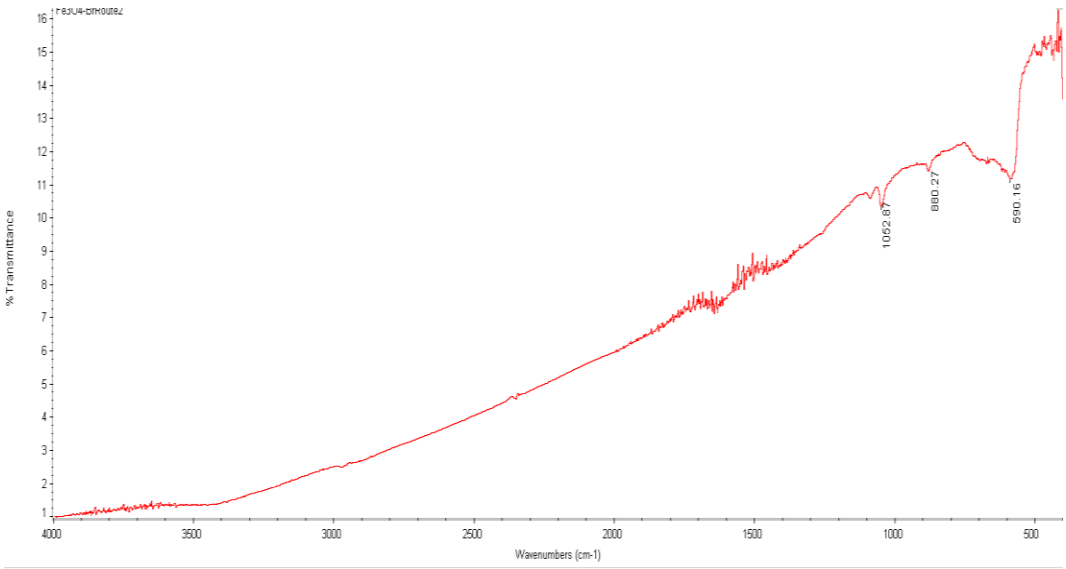

Figure A 5 An confirmation of FMNCs-Br by FTIR spectrum.

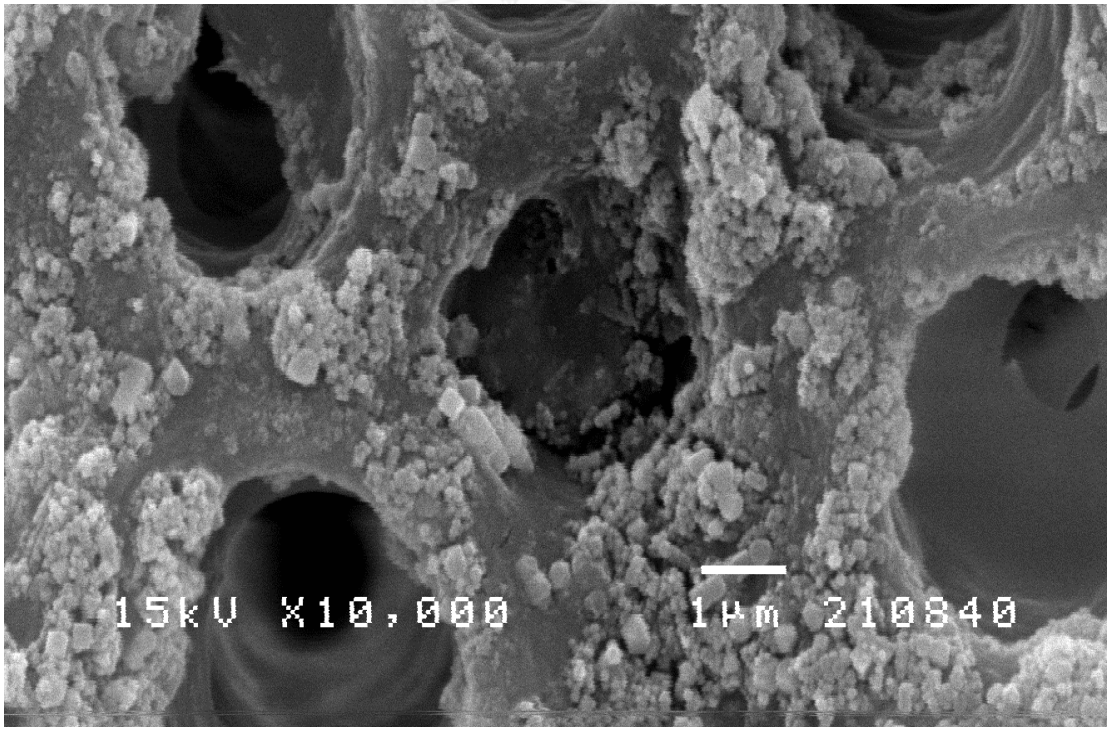

Figure A 6 A detailed photograph of FMNCs/PDMAEMA infiltrated through dentin discs.

VITA

Mr. Phranot Ajkidkarn was born on April 10, 1991 in Lopburi, Thailand. He graduated in Bachelor Degree of Science in Applied Chemistry International program from Chulalongkorn University in 2013. He continued his Master's Degree of Science in Petrochemistry and Polymer Science at Chulalongkorn University. He became a member of Materials Chemistry and Catalysis Research Unit under the supervision of Dr. Numpon Insin. On 9-11 Febuary 2016, He attended the 16th Pure and Applied Chemistry International Conference 2016 in the title of "SYNTHESIS OF FERRIMAGNETIC MAGNETITE NANOCUBES COATED WITH POLY(2-(DIMETHYLAMINO)ETHYL METHACRYLATE) FOR APPLICATIONS IN DRUG DELIVERY IN DENTISTRY" by poster presentation. Moreover, he participated the 11th International Conference on the Scientific and Clinical Applications of Magnetic Carriers on May 31 - June 4, 2016 in the title of "SYNTHESIS, CHARACTERIZATION, DRUG RELEASE AND TRANSDENTINAL DELIVERY STUDIES OF MAGNETIC NANOCUBES COATED WITH BIODEGRADABLE POLY(2- (DIMETHYL AMINO)ETHYL METHACRYLATE)" by poster presentation.

E-mail address: phranot_ajk@hotmail.com